

Figure 4 Mechanical-stretch-stimulated production of inositol phosphates through the AT1 receptor. COS7 cells (–) or COS7 cells transfected with AT1-WT (WT) were labelled with myo-[³H]inositol 24 h after transfection. After 24 h of labelling, cells were incubated with vehicle (–) or candesartan (Can) for 5 h at 37 °C. The accumulation of inositol phosphates was measured as described in Methods. Some COS7 cells transiently transfected with AT1-WT (WT) were subjected to stretching (St) for 45 min or no stimulus (–) in the presence of 5 mM LiCl. **P* < 0.05.

The AT1 receptor is a guanine-nucleotide-binding protein (G-protein)-coupled receptor (GPCR), a member of a large family of cell-surface receptors that contain common structural features characterized by seven transmembrane helices essential for signal transduction^{15–17}. Activation of other GPCRs, such as the receptors of endothelin 1 (ET-1) and catecholamines, also induces cardiomyocyte hypertrophy^{18,19}. We therefore tested whether mechanical stretch can activate these receptors in a ligand-independent manner. We stretched COS7 cells overexpressing either the wild-type ET-1 type A (ET1A) receptor (Fig. 2g) or the wild-type β 2-adrenoceptor (β 2-AR; Fig. 2h). Whereas ET-1 and isoproterenol (ISO) activated ERKs, mechanical stretch did not evoke significant activation of ERKs in these transfected cells. These results suggest that the activation of GPCRs by mechanical stretch without the involvement of their ligands is not a general phenomenon but specific to some GPCRs including the AT1 receptor.

G proteins and Jak2 are activated by stretch

As a member of the GPCR family, the AT1 receptor evokes intracellular signals through G proteins^{20,21}. We therefore examined whether mechanical stress could activate G proteins through the AT1 receptor. Stimulation with either AII or mechanical stretch induced the redistribution of G_{αq11} subunits into the cytosol of HEK293-AT1-WT cells and this redistribution was inhibited by pretreatment with candesartan (Fig. 3a), suggesting that G_{αq11} is activated by mechanical stretch as well as by AII.

To determine whether an interaction between the AT1 receptor and G proteins has a role in the activation of ERKs, we transfected an AT1 receptor mutant that does not couple to G proteins (AT1-i2m)²² into COS7 cells. Activation of ERKs by mechanical stretch was weaker in the AT1-i2m-transfected cells than in those overexpressing AT1-WT (Fig. 3b), suggesting that coupling of G proteins to the AT1 receptor is partly involved in the stretch-induced activation of ERKs.

Non-receptor-type tyrosine kinases such as the Janus kinase (Jak) family and the Src family may be important in AT1 receptor

signalling^{22,23}. The AT1 receptor activates the Src–Ras–ERK pathway independently of G-protein coupling through the association and activation of Jak2 (refs 22,24,25). Mechanical stretch induced association of Jak2 with the AT1 receptor (Fig. 3c) and phosphorylation of Jak2 (Fig. 3d) in HEK293-AT1-WT cells. Pretreatment of the cells with candesartan significantly suppressed association with the AT1 receptor and phosphorylation of Jak2 (Fig. 3c, d). Mechanical stretch did not activate ERKs in HEK293-AT1-WT cells that had been pretreated with AG490, a specific inhibitor of Jak2 (Fig. 3e), or in COS7 cells expressing an AT1-mutant (AT1-mut2)²⁵ that lacks a binding domain for Jak2 (Fig. 3f). These results suggest that activation of Jak2 is crucially involved in the stretch-induced activation of ERKs.

Mechanical stretch upregulates inositol phosphates

To identify other stretch-induced events, we examined the accumulation of inositol phosphates in COS-7 cells expressing AT1-WT. Overexpression of AT1-WT resulted in a roughly fivefold increase in basal inositol phosphates, as compared with untransfected cells (Fig. 4). Mechanical stretch of these AT1-WT-expressing cells further upregulated inositol phosphate production by about twofold (Fig. 4). Stretching the parental COS7 cells did not increase inositol phosphate production (data not shown). Candesartan inhibited the accumulation of inositol phosphates in COS7 cells expressing AT1-WT, as well as the stretch-induced increase in inositol phosphate production (Fig. 4).

Load-induced cardiac hypertrophy through AT1 receptor

We examined whether mechanical stress could induce cardiac hypertrophy *in vivo* through the AT1 receptor in the absence of AII. We imposed a pressure overload on the heart by constricting the transverse aorta (TAC) of adult male *ATG*^{–/–} mice. Pressure overload for 2 weeks induced significant hypertrophy in the heart of the *ATG*^{–/–} mice (Fig. 5a, b). Heart weight was increased from 110 ± 12 mg to 189 ± 14 mg after 2 weeks of pressure overload (Fig. 5b).

Although treatment with candesartan did not reduce blood pressure in the right carotid artery (sham operated, 78 ± 10 mmHg; TAC plus saline, 166 ± 15 mmHg; TAC plus candesartan, 160 ± 17 mmHg), the development of cardiac hypertrophy was significantly attenuated by candesartan (heart weight, 145 ± 21 mg; Fig. 5). These results suggest that mechanical stress can induce cardiac hypertrophy *in vivo* by activating the AT1 receptor without the involvement of AII.

DISCUSSION

Many basic and clinical studies have shown that RAS is crucially involved in the development of various cardiovascular diseases^{9–12}. Much evidence has indicated that RAS exists in various organs, as well as in the circulation, and that local RAS has an important role in organ damage including cardiac hypertrophy^{26,27}. All components of RAS, such as angiotensinogen, renin, angiotensin-converting enzyme and receptors, are present in the heart^{26,27}, and AII induces hypertrophy of cultured cardiomyocytes²⁷. It has been reported that AII is stored in cardiomyocytes and that mechanical stretch induces the secretion of stored AII into the culture medium, resulting in the induction of cardiomyocyte hypertrophy by the autocrine mechanism⁶. Taking these observations together, haemodynamic overload has been thought to promote cardiac hypertrophy by inducing the secretion of AII in the heart. In this study, however, we have shown that mechanical stress can induce cardiomyocyte hypertrophy both *in vitro* and *in vivo* through the AT1 receptor without the involvement of AII.

Although mechanical stretch has been reported to induce the release of endogenous AII from cardiomyocytes⁶, by radioimmunoassay we did not detect a significant increase in AII in the cul-

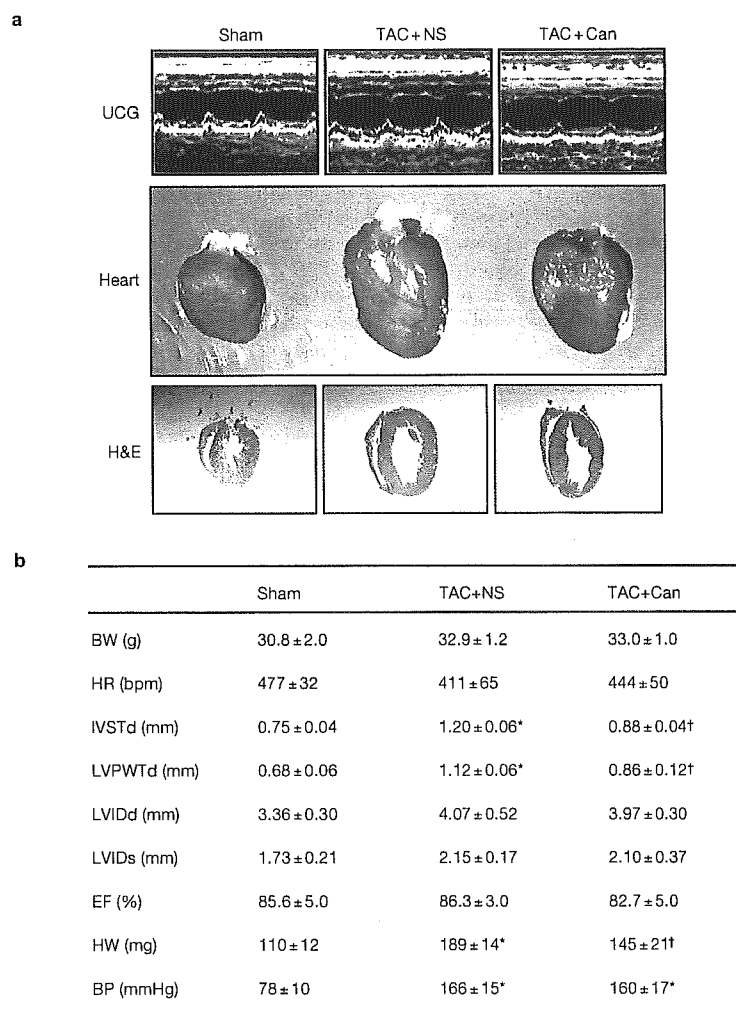


Figure 5 Cardiac hypertrophy in *ATG*^{-/-} mice induced by pressure overload. Ten-week-old male *ATG*^{-/-} mice, treated with saline (NS) or candesartan (Can), were subjected to a sham or TAC operation. Echocardiography and catheterization were done 2 weeks later. (a) Top, M-mode echocardiograms; middle, gross appearance of the heart; bottom, sections stained by H&E. (b) Echocardiographic results and

haemodynamic parameters, shown as the mean ± s.e.m. ($n = 3$). * $P < 0.05$ versus sham operated; † $P < 0.05$ versus saline. BW, body weight; HR, heart rate; IVSTd, thickness of interventricular septum at diastole; LVPWTd, posterior wall thickness of LV at diastole; LVIDd and LVIDs, LV internal dimension at end diastole and systole, respectively; EF, ejection fraction; HW, heart weight; BP, systolic blood pressure.

ture medium after stretch. AII concentration varied considerably in the conditioned media, whereas the degree of ERK activation induced by stretch was constant, which also suggests that secreted AII is not involved in the stretch-induced activation of ERKs. A very sensitive bioassay, as well as radioimmunoassay, showed that the concentration of AII in medium conditioned by stretch was less than 10^{-11} M, which is far too low to evoke a hypertrophic response in cardiomyocytes. The reason for the difference in the role of secreted AII by stretch between the previous report⁶ and this study is not clear at present. Many reports have shown that cardiomyocytes contain about 10^{-13} mol of AII per gram of cells^{28–30}. Thus, even if all of the AII stored in cardiomyocytes were secreted by stretch, at most about 10^{-11} M AII would be detected in the culture medium. We detected roughly 2×10^{-12} M AII in culture medium conditioned by stretch for 8 min, consistent with the theoretical concentrations.

Although it is evident that mechanical stress is the primary trigger of cardiac hypertrophy, it is not clear how mechanical stress is received and converted into the active intracellular signalling responsible for the development of cardiac hypertrophy. Muscle LIM protein, integrins and their associated signalling machinery have been reported to be sensors for mechanical stress^{31,32}. We propose that the AT1 receptor is also a receptor for mechanical stress. Mechanical stretch did not activate ERKs in HEK293 cells or COS7 cells, but expression of the AT1 receptor gave these cells the ability to respond to stretch. Bioassays using conditioned medium and RT-PCR analysis showed that there is little or no AII in HEK293 cells or COS7 cells. These results suggest that the AT1 receptor is a 'mechanical sensor' and converts mechanical stress into biochemical signals inside the cells.

This hypothesis was confirmed by results from cells expressing the AT1-mut1, which cannot bind AII, and from cardiomyocytes pre-

pared from *ATG*^{-/-} mice. Although AII did not activate ERKs in cells expressing AT1-mut1, mechanical stretch activated ERKs in these cells and this activation was inhibited by an AT1 receptor blocker, candesartan. Mechanical stretch activated ERKs in cardiomyocytes prepared from *ATG*^{-/-} mice, which do not express AII, and candesartan inhibited this activation.

Because mechanical stretch did not activate ERKs in cells expressing the ET1A or β 2-AR receptors, not all GPCRs are necessarily a mechanical sensor. Although we do not know at present why the AT1 receptor, but not the ET1A or β 2-AR receptor, is significantly activated by mechanical stretch, there are a few possibilities. First, specificity may be due to molecules that associate with the AT1 receptor. We found that in the response to mechanical stretch, some unknown molecules bind to the AT1 receptor (our own unpublished results). Second, diversity in the structures and expression of the receptors may also determine their responsibility to mechanical stress^{16,27,33}.

After binding to AII, the AT1 receptor changes its conformation into an active form and stimulates G proteins through its intracellular domains^{15,20,33,34}. The intracellular loops and the region between residues 312 and 318 in the carboxy-terminal tail of the AT1 receptor have been reported to be essential for coupling and activating G proteins³⁵. After activation, G proteins dissociate into α - and $\beta\gamma$ -subunits, and the α -subunit is translocated into the cytosol³⁴. In addition, ligand binding to the AT1 receptor induces association of the C terminus of the AT1 receptor with Jak2, thereby resulting in activation of the Jak2-STAT3 pathway²²⁻²⁵. Although there is no direct evidence, our results suggest that, similar to AII binding to the AT1 receptor, mechanical stress induces a conformational change in the AT1 receptor by a mechanism independent of AII binding, resulting in the association and activation of G proteins and Jak2.

There are a few mechanisms by which mechanical stress might activate the AT1 receptor without the involvement of AII. First, stretching the cell membrane may directly change the conformation of the AT1 receptor. Many receptors can change their conformation between the active and inactive state under basal conditions without ligands^{36,37}. Candesartan reduced the basal activity of ERKs, suggesting that part of the wild-type AT1 receptor is in an active state, and mechanical stress may increase the number of AT1 receptors in the active state. Second, mechanical stretch might activate specific mechanical sensors, which then activate the AT1 receptor from inside the cells. Potential stretch sensors, such as muscle LIM protein, integrins and stretch-sensitive ion channels, might activate the AT1 receptor, though the underlying mechanism remains to be determined.

Strong pressure overload induced cardiac hypertrophy in *ATG*^{-/-} mice, indicating that mechanical stress can induce cardiac hypertrophy without AII. Treatment with candesartan significantly attenuated the development of cardiac hypertrophy without reducing blood pressure, suggesting that mechanical stress activates the AT1 receptor and induces cardiac hypertrophy without the involvement of AII *in vivo*. We previously reported that pressure overload induces cardiac hypertrophy in AT1a receptor knockout mice³⁸. The activity of tyrosine kinases is upregulated before stretch and more strongly enhanced by mechanical stretch in AT1a-receptor-deficient cardiomyocytes as compared with wild-type cells through epidermal growth factor (EGF) receptor tyrosine kinases³⁹, suggesting that the AT1 receptor is not indispensable for stretch-induced cardiac hypertrophy and that some compensatory mechanisms operate and induce cardiac hypertrophy even in the absence of the AT1 receptor^{38,39}.

Candesartan reduced the basal activity of ERKs and inositol phosphates in cells overexpressing AT1-WT and inhibited the

stretch-induced activation of ERKs and increase in inositol phosphates independently of AII, suggesting that candesartan works as an inverse agonist of the AT1 receptor. An inverse agonist of the AT1 receptor is defined as an agent that stabilizes the AT1 receptor in an inactive conformation, thereby inhibiting signals evoked by the wild-type or active AT1 receptor. As an inverse agonist, candesartan may inhibit changes in conformation of AT1 receptor and thus may efficiently suppress its activation induced by both mechanical stress and AII. Much evidence suggests that local RAS has a crucial role in injury to various organs^{26,27,40}. It remains to be determined whether activation of the AT1 receptor without AII occurs in other organs, and whether inverse agonists prevent organ damage more effectively than do competitive antagonists. □

METHODS

cDNA constructs. The AT1a receptor mutants lacking binding activity with AII (AT1-mut1) or the Jak2 coupling domain (AT1-mut2) were generated by PCR from the wild-type mouse AT1 receptor (GenBank accession number S37484)⁴¹ by replacement of Lys 199 with glutamine¹³ or truncation of the C terminus (residues 312–359)²², respectively. AT1-i2m²², β 2-AR⁴² and ET1A⁴³ were gifts from J. Sadoshima, R. J. Lefkowitz and S. Kimura, respectively. The complementary DNAs used in this study are summarized in Supplementary Information, Table 1.

Cell culture and transfection. We prepared primary cultures of cardiomyocytes from the ventricles of 1-day-old Wistar rats or *ATG*^{-/-} mice as described¹⁹. Adult and neonatal cardiomyocytes of *ATG*^{-/-} mice were prepared as described⁴⁴. HEK293 and COS7 cells were cultured in Dulbecco's modified Eagle's medium with 10% serum. cDNAs were transfected by the calcium phosphate method as described¹⁹. Stable transformants were selected by the addition of hygromycin B to the cells 3 d after transfection and for all subsequent passages of the cells⁴¹. All cultures were transferred to serum-free conditions 48 h before stimulation.

Western blotting. Total proteins (50 μ g) were size-fractionated by SDS-PAGE and transferred to Immobilon-P membranes (Millipore). The blotted membranes were incubated with antibodies against phosphorylated ERKs, phosphorylated Jak2, Jak2, AT1 or G α q11 (Santa Cruz).

ATG gene expression. Expression of the *ATG* gene was examined by RT-PCR using specific primers (sense, 5'-TTCAGGCCAAGACCTCCC-3'; antisense, 5'-CCAGC-CGGGAGGTGCAGT-3')⁴⁵. We separated the PCR products on 1.2% agarose gels and visualized them by using ethidium bromide.

Detection of inositol phosphates. Accumulation of inositol phosphates was assayed in COS7 cells as described^{46,47}. In brief, 24 h after transfection by the DEAE-adenovirus method⁴⁸, cells were replated in 24-well plates at 1.5×10^5 cells per well and labelled for 24 h with myo-[³H]inositol (2 μ Ci ml⁻¹; Amersham). The cells were washed in medium containing 5 mM LiCl for 10 min, incubated with vehicle or candesartan for 5 h, and then subjected to mechanical stretch for 45 min in the presence of 5 mM LiCl. Inositol phosphates and total inositol fractions were resolved on a Dowex AG 1-X8 formate column (Bio-Rad), and inositol phosphate accumulation was estimated by determining the ratio of inositol phosphate radioactivity to the sum of inositol phosphate plus inositol radioactivity.

AII in the medium of cultured cardiomyocytes. Culture medium (2 ml per dish) was collected from dishes before and after stretching the cells by 20% for 8 min. We measured AII concentration by radioimmunoassay using two antibodies specific for AII (SRL Co.).

TAC operation. TAC operation was done on 10-week-old male *ATG*^{-/-} mice and wild-type C52/BL6 mice⁴⁴. A mini-osmotic pump (Alzet) filled with saline or candesartan was implanted subcutaneously in mice 3 d before TAC. All mouse protocols were approved by the guidelines of Chiba University.

Haemodynamic parameters. Transthoracic echocardiography (UCG) was done as reported³⁸ using a Agilent sonos 4500 (Agilent Technologies Co.) equipped

with a 11-MHz imaging transducer. Haemodynamic measurements were taken by inserting a micromanometer catheter (Millar 1.4F, SPR 671, Millar Instruments) from the right common carotid artery into the aorta and then the left ventricle (LV). The transducer was connected to the MacLab system (AD Instruments) to record the pressure. For heart morphometry, hearts were perfused with 10% buffered formalin and subsequently embedded in paraffin, sectioned and stained with haematoxylin and eosin (H&E).

Statistics. Data are shown as mean \pm s.e.m. Multiple group comparison was done by a one-way analysis of variance (ANOVA), followed by the Bonferroni procedure for comparison of means. A two-tailed Student's *t*-test was used to compare drug-treated and vehicle-treated specimens under identical conditions. Values of $P < 0.05$ were considered statistically significant.

Note: Supplementary Information is available on the Nature Cell Biology website.

ACKNOWLEDGEMENTS

We thank R. J. Lefkowitz, J. Sadoshima and S. Kimura for plasmids; S.-i. Miura for advice; and A. Okubo, E. Fujita, R. Kobayashi and M. Watanabe for technical support. This work was supported by a Grant-in-Aid for Scientific Research, Developmental Scientific Research, and Scientific Research on Priority Areas from the Ministry of Education, Science, Sports, and Culture; and by a grant for research on life science from Uehara Memorial Foundation, Japan (to I.K.).

COMPETING FINANCIAL INTERESTS

The authors declare that they have no competing financial interests.

Received 25 March 2004; accepted 19 April 2004

Published online at <http://www.nature.com/naturecellbiology>.

- Levy, D., Garrison, R. J., Savage, D. D., Kannel, W. B. & Castelli, W. P. Prognostic implications of echocardiographically determined left ventricular mass in the Framingham heart study. *N. Eng. J. Med.* **322**, 1561–1566 (1990).
- Chien, K. R., Grace, A. A. & Hunter, J. J. Molecular biology of cardiac hypertrophy and heart failure. In *Molecular Basis of Cardiovascular Disease* (ed. K. R. Chien) 211–250 (W. B. Saunders, Philadelphia, PA, 1998).
- Komuro, I. *et al.* Stretching cardiac myocytes stimulates protooncogene expression. *J. Biol. Chem.* **265**, 3595–3598 (1990).
- Sadoshima, J., Jahn, L., Takahashi, T., Kulik, T. J. & Izumo, S. Molecular characterization of the stretch-induced adaptation of cultured cardiac cells. An *in vitro* model of load-induced cardiac hypertrophy. *J. Biol. Chem.* **267**, 10551–10560 (1992).
- Komuro, I. & Yazaki, Y. Control of cardiac gene expression by mechanical stress. *Annu. Rev. Physiol.* **55**, 55–75 (1993).
- Sadoshima, J., Xu, Y., Slayter, H. S. & Izumo, S. Autocrine release of angiotensin II mediates stretch-induced hypertrophy of cardiac myocytes *in vitro*. *Cell* **75**, 977–984 (1993).
- Yamazaki, T. *et al.* Angiotensin II partly mediates mechanical stress-induced cardiac hypertrophy. *Circ. Res.* **77**, 258–265 (1995).
- Kojima, M. *et al.* Angiotensin II receptor antagonist TCV-116 induces regression of hypertensive left ventricular hypertrophy *in vivo* and inhibits the intracellular signaling pathway of stretch-mediated cardiomyocyte hypertrophy *in vitro*. *Circulation* **89**, 2204–2211 (1994).
- Griendling, K. K., Lassegue, B. & Alexander, R. W. Angiotensin receptors and their therapeutic implications. *Annu. Rev. Pharmacol. Toxicol.* **36**, 281–306 (1996).
- Pitt, B. *et al.* Effect of losartan compared with captopril on mortality in patients with symptomatic heart failure: randomised trial—the Losartan Heart Failure Survival Study ELITE II. *Lancet* **355**, 1582–1587 (2000).
- Cohn, J. N. *et al.* A randomized trial of the angiotensin-receptor blocker valsartan in chronic heart failure. *N. Eng. J. Med.* **345**, 1667–1675 (2001).
- Lindholm, L. H. *et al.* Cardiovascular morbidity and mortality in patients with diabetes in the Losartan Intervention For Endpoint reduction in hypertension study (LIFE): a randomised trial against atenolol. *Lancet* **359**, 1004–1010 (2002).
- Yamano, Y., Ohyama, K., Chaki, S., Guo, D. F. & Inagami, T. Identification of amino acid residues of rat angiotensin II receptor for ligand binding by site directed mutagenesis. *Biochem. Biophys. Res. Comm.* **187**, 1426–1431 (1992).
- Tanimoto, K. *et al.* Angiotensinogen-deficient mice with hypotension. *J. Biol. Chem.* **269**, 31334–31337 (1994).
- van Biesen, T., Luttrell, L. M., Hawes, B. E. & Lefkowitz, R. J. Mitogenic signaling via G protein-coupled receptors. *Endocr. Rev.* **17**, 698–714 (1996).
- Rockman, H. A., Koch, W. J. & Lefkowitz, R. J. Seven-transmembrane-spanning receptors and heart function. *Nature* **415**, 206–212 (2002).
- Bockaert, J. & Pin, J. P. Molecular tinkering of G protein-coupled receptors: an evolutionary success. *EMBO J.* **18**, 1723–1729 (1999).
- Yamazaki, T. *et al.* Endothelin-1 is involved in mechanical stress-induced cardiomyocyte hypertrophy. *J. Biol. Chem.* **271**, 3221–3228 (1996).
- Zou, Y. *et al.* Both G_s and G_i proteins are critically involved in isoproterenol-induced cardiomyocyte hypertrophy. *J. Biol. Chem.* **274**, 9760–9770 (1999).
- Bernstein, K. E. & Alexander, R. W. Counterpoint: molecular analysis of the angiotensin II receptor. *Endocr. Rev.* **13**, 381–386 (1992).
- Inagami, T. Molecular biology and signaling of angiotensin receptors: an overview. *J. Am. Soc. Nephrol.* **11**, S2–S7 (1999).
- Seta, K., Nanamori, M., Modrall, J. G., Neubig, R. R. & Sadoshima, J. AT1 receptor mutant lacking heterotrimeric G protein coupling activates the Src-Ras-ERK pathway without nuclear translocation of ERKs. *J. Biol. Chem.* **277**, 9268–9277 (2002).
- Marrero, M. B. *et al.* Direct stimulation of Jak/STAT pathway by the angiotensin II AT1 receptor. *Nature* **375**, 247–250 (1995).
- Ali, M. S. *et al.* Dependence on the motif YIPP for the physical association of Jak2 kinase with the intracellular carboxyl tail of the angiotensin II AT1 receptor. *J. Biol. Chem.* **272**, 23382–23388 (1997).
- Ali, M. S., Sayeski, P. P. & Bernstein, K. E. Jak2 acts as both a STAT1 kinase and as a molecular bridge linking STAT1 to the angiotensin II AT1 receptor. *J. Biol. Chem.* **275**, 15586–15593 (2000).
- Lee, M. A., Bohm, M., Paul, M. & Ganten, D. Tissue renin-angiotensin systems. Their role in cardiovascular disease. *Circulation* **87**, 7–13 (1993).
- Baker, K. M., Booz, G. W. & Dostal, D. E. Cardiac actions of angiotensin II: role of an intracardiac renin-angiotensin system. *Annu. Rev. Physiol.* **54**, 227–241 (1992).
- Mazzolai, L. *et al.* Increased cardiac angiotensin II levels induce right and left ventricular hypertrophy in normotensive mice. *Hypertension* **35**, 985–991 (2000).
- Wei, C. C. *et al.* Differential ANG II generation in plasma and tissue of mice with decreased expression of the ACE gene. *Am. J. Physiol.* **282**, H2254–H2258 (2002).
- Campbell, D. J. *et al.* Effect of reduced angiotensin-converting enzyme gene expression and angiotensin-converting enzyme inhibition on angiotensin and bradykinin peptide levels in mice. *Hypertension* **43**, 1–6 (2004).
- Knoll, R. *et al.* The cardiac mechanical stretch sensor machinery involves a Z disc complex that is defective in a subset of human dilated cardiomyopathy. *Cell* **111**, 943–955 (2002).
- Brancaccio, M. *et al.* Melusin, a muscle-specific integrin β 1-interacting protein, is required to prevent cardiac failure in response to chronic pressure overload. *Nature Med.* **9**, 68–75 (2003).
- Karnik, S. S., Gogonea, C., Patil, S., Saad, Y. & Takezako, T. Activation of G-protein-coupled receptors: a common molecular mechanism. *Trends Endocrinol. Metab.* **14**, 431–437 (2004).
- Akhter, S. A. *et al.* Targeting the receptor-G_q interface to inhibit *in vivo* pressure overload myocardial hypertrophy. *Science* **280**, 574–577 (1998).
- Sano, T. *et al.* A domain for G protein coupling in carboxyl-terminal tail of rat angiotensin II receptor type 1A. *J. Biol. Chem.* **272**, 23631–23636 (1997).
- Lefkowitz, R. J., Cotecchia, S., Samama, P. & Costa, T. Constitutive activity of receptors coupled to guanine nucleotide regulatory proteins. *Trends Pharmacol. Sci.* **14**, 303–307 (1993).
- Leurs, R., Smit, M. J., Alewijnse, A. E. & Timmerman, H. Agonist-independent regulation of constitutively active G-protein-coupled receptors. *Trends Biochem. Sci.* **23**, 418–422 (1998).
- Harada, K. *et al.* Acute pressure overload could induce hypertrophic responses in the heart of angiotensin II type 1a knockout mice. *Circ. Res.* **82**, 779–785 (1998).
- Kudoh, S. *et al.* Mechanical stretch induces hypertrophic responses in cardiac myocytes of angiotensin II type 1a receptor knockout mice. *J. Biol. Chem.* **273**, 24037–24043 (1998).
- Bader, M. *et al.* Tissue renin-angiotensin systems: new insights from experimental animal models in hypertension research. *J. Mol. Med.* **79**, 76–102 (2001).
- Ishida, J. *et al.* Expression and characterization of mouse angiotensin II type 1a receptor tagging hemagglutinin epitope in cultured cells. *Int. J. Mol. Med.* **3**, 263–270 (1999).
- Daaka, Y., Luttrell, L. M. & Lefkowitz, R. J. Switching of the coupling of the β 2-adrenergic receptor to different G proteins by protein kinase A. *Nature* **390**, 88–91 (1997).
- Sakurai, T. *et al.* Cloning of a cDNA encoding a non-isopeptide-selective subtype of the endothelin receptor. *Nature* **348**, 732–735 (1990).
- Sambrano, G. R. *et al.* Navigating the signalling network in mouse cardiac myocytes. *Nature* **420**, 712–714 (2002).
- Malhotra, R., Sadoshima, J., Brosius, F. C. & Izumo, S. Mechanical stretch and angiotensin II differentially upregulated the renin-angiotensin system in cardiac myocytes *in vitro*. *Circ. Res.* **85**, 137–146 (1999).
- Conklin, B. R., Chabre, O., Wong, Y. H., Federman, A. D. & Bourne, H. R. Recombinant G_q α . Mutational activation and coupling to receptors and phospholipase C. *J. Biol. Chem.* **267**, 31–34 (1992).
- Iiri, T., Bell, S. M., Baranski, T. J., Fujita, T. & Bourne, H. R. A G_q α mutant designed to inhibit receptor signaling through Gs. *Proc. Natl. Acad. Sci. USA* **96**, 499–504 (1999).
- Garcia, P. D., Onrust, R., Bell, S. M., Sakmar, T. P. & Bourne, H. R. Transducin- α C-terminal mutations prevent activation by rhodopsin: a new assay using recombinant proteins expressed in cultured cells. *EMBO J.* **14**, 4460–4469 (1995).

Akt negatively regulates the *in vitro* lifespan of human endothelial cells via a p53/p21-dependent pathway

Hideyuki Miyauchi¹, Tohru Minamino¹,
Kaoru Tateno, Takeshige Kunieda,
Haruhiro Toko and Issei Komuro*

Department of Cardiovascular Science and Medicine, Chiba University Graduate School of Medicine, Chuo-ku, Chiba, Japan

The signaling pathway of insulin/insulin-like growth factor-1/phosphatidylinositol-3 kinase/Akt is known to regulate longevity as well as resistance to oxidative stress in the nematode *Caenorhabditis elegans*. This regulatory process involves the activity of DAF-16, a forkhead transcription factor. Although reduction-of-function mutations in components of this pathway have been shown to extend the lifespan in organisms ranging from yeast to mice, activation of Akt has been reported to promote proliferation and survival of mammalian cells. Here we show that Akt activity increases along with cellular senescence and that inhibition of Akt extends the lifespan of primary cultured human endothelial cells. Constitutive activation of Akt promotes senescence-like arrest of cell growth via a p53/p21-dependent pathway, and inhibition of forkhead transcription factor FOXO3a by Akt is essential for this growth arrest to occur. FOXO3a influences p53 activity by regulating the level of reactive oxygen species. These findings reveal a novel role of Akt in regulating the cellular lifespan and suggest that the mechanism of longevity is conserved in primary cultured human cells and that Akt-induced senescence may be involved in vascular pathophysiology.

The EMBO Journal (2004) 23, 212–220. doi:10.1038/sj.emboj.7600045; Published online 8 January 2004

Subject Categories: cell cycle; molecular biology of disease
Keywords: aging; Akt; endothelial cells; senescence

Introduction

Cellular senescence is the limited ability of primary human cells to divide when cultured *in vitro* and is accompanied by a specific set of changes in cell morphology, gene expression and function. These phenotypic changes have been implicated in human aging (Faragher and Kipling, 1998). This hypothesis, the cellular hypothesis of aging, was established by Hayflick (1975) and is supported by evidence that the replicative potential of primary cultured human cells is dependent on

donor age and that the growth potential of cultured cells correlates well with the mean maximum lifespan of the species from which the cells are derived (Rohme, 1981), although some conflicting data have been reported (Cristofalo *et al*, 1998). Primary cultured cells obtained from patients with premature aging syndromes, such as Werner syndrome and Bloom syndrome, are known to have a shorter lifespan than the cells from age-matched healthy populations (Rohme, 1981; Thompson and Holliday, 1983), further supporting this hypothesis. Cell division is essential for the survival of multicellular organisms that contain renewable tissues, but also places the organism at the risk of developing cancer. It has been suggested that complex organisms have evolved at least two cellular mechanisms to prevent oncogenic transformation, which are apoptosis and cellular senescence (Campisi, 2001). Accordingly, age-associated diseases could be regarded as a by-product of the tumor suppressor mechanism, cellular senescence (Weinstein and Ciszek, 2002).

Many molecular mechanisms have been suggested to contribute to human aging and its associated diseases. Recent genetic analyses have demonstrated that reduction-of-function mutations in the signaling pathway of insulin/insulin-like growth factor-1 (IGF-1)/phosphatidylinositol-3 kinase (PI3K)/Akt (also known as protein kinase B) extend the longevity of the nematode *Caenorhabditis elegans* (Kenyon *et al*, 1993; Morris *et al*, 1996; Paradis and Ruvkun, 1998; Guarente and Kenyon, 2000; Kenyon, 2001; Lee *et al*, 2001; Lin *et al*, 2001; Longo and Finch, 2003). The forkhead transcription factor DAF-16, which is phosphorylated and thereby inactivated by Akt (Lee *et al*, 2001; Lin *et al*, 2001), plays an essential role in this longevity pathway (Lin *et al*, 1997; Ogg *et al*, 1997). More recently, it has been reported that the genes regulating longevity are conserved in organisms ranging from yeast to mice. Mutation of *Sch9*, which is homologous to Akt, extends the lifespan of yeast (Fabrizio *et al*, 2001), and mutations that decrease the activity of the insulin/IGF-1-like pathway increase the longevity of fruit flies (Tatar *et al*, 2001) and mice (Bluhner *et al*, 2003; Holzenberger *et al*, 2003). These mutations that extend the lifespan are associated with increased resistance to oxidative stress, which is partly mediated by the increased expression of antioxidant genes (Honda and Honda, 1999; Fabrizio *et al*, 2003; Murphy *et al*, 2003).

In mammalian cells, activation of Akt has been reported to induce proliferation and survival, thereby promoting tumorigenesis (Datta *et al*, 1999; Blume-Jensen and Hunter, 2001; Testa and Bellacosa, 2001). Overexpression of Akt can transform NIH3T3 cells (Cheng *et al*, 1997), while introduction of Akt antisense RNA inhibits the tumorigenic phenotype of cancer cells expressing high levels of Akt (Cheng *et al*, 1996). The mechanisms by which Akt promotes cell proliferation and survival are likely to be multifactorial, because it has been reported to directly phosphorylate several components of the cell cycle machinery as well as the cell death machinery (Datta *et al*, 1999). Akt counteracts the effect of

*Corresponding author. Department of Cardiovascular Science and Medicine, Chiba University Graduate School of Medicine, 1-8-1 Inohana, Chuo-ku, Chiba 260-8670, Japan. Tel.: +81 43 226 2097; Fax: +81 43 226 2557; E-mail: komuro-tky@umin.ac.jp

¹These authors contributed equally to this work

Received: 25 June 2003; accepted: 25 November 2003; Published online: 8 January 2004

cyclin-dependent kinase inhibitors on cell cycle progression by modulating their intracellular localization and level of transcription (Medema *et al.*, 2000; Shin *et al.*, 2002; Viglietto *et al.*, 2002; Zhou *et al.*, 2001a). Akt also increases the cyclin D1 level by inhibiting its degradation, which is important in the G1/S phase transition (Diehl *et al.*, 1998). Moreover, it is known that Akt phosphorylates and inactivates proapoptotic factors such as BAD (Datta *et al.*, 1997; del Peso *et al.*, 1997) and procaspase-9 (Cardone *et al.*, 1998), thereby promoting cell survival. Although these reports have suggested an important role of Akt in human malignancy (Blume-Jensen and Hunter, 2001; Testa and Bellacosa, 2001), it has mainly been examined in immortal cell lines and the impact of Akt activation on the growth and lifespan of primary cultured human cells is unknown.

In the present study, we found that inhibition of Akt could prolong the lifespan of primary cultured human endothelial cells, whereas constitutive activation of Akt promoted senescence-like growth arrest via a p53/p21-dependent pathway. Akt-induced growth arrest was inhibited by a mutated forkhead transcription factor that was resistant to Akt phosphorylation. These findings disclose a novel role of Akt in regulating the lifespan of cells and suggest that the mechanism of longevity is conserved in primary cultured human cells.

Results

Akt activation reduces the lifespan of human endothelial cells

We first investigated whether Akt activity was associated with cellular senescence of primary cultured human endothelial cells. Senescent endothelial cells had higher phospho-Akt levels than young endothelial cells (Figure 1A). To assess the actual role of Akt activity in regulating cellular lifespan, we infected primary cultured human endothelial cells with a retroviral vector encoding either constitutively activated myc-tagged Akt (AktCA) or dominant-negative myc-tagged Akt (AktDN). The empty retroviral vector pLNCX (Mock), encoding a neomycin resistance gene alone, was also transduced into endothelial cells as a control. Infected cells were purified using G418 for 7 days and then recultured until the cells underwent senescence. The 8th day after infection is designated as day 0 in all of the following experiments. Western blot analysis with anti-c-Myc antibody and anti-Akt antibody demonstrated that both AktCA and AktDN proteins were expressed by the endothelial cells, showing an approximately 4- to 8-fold increase of total Akt protein compared to endogenous Akt protein (Figure 1B). Long-term culture studies showed that constitutive activation of Akt significantly shortened the lifespan of the endothelial cells, whereas inhibition of Akt activity delayed senescence compared with mock-infected cells (Figure 1B). Introduction of AktDN influenced cellular lifespan in the late passages, but not in the early passages, suggesting that Akt activity increased with further cell division and thus promoted senescence. Expression of AktCA markedly reduced cell growth by day 7 (Figure 1C). AktCA-transduced endothelial cells were flattened and enlarged, while mock- or AktDN-infected endothelial cells exhibited normal morphology and growth (Figures 1C and D). Senescence-associated β -galactosidase activity was also increased in AktCA-transduced cells (Figure 1D). These changes of the phenotype, which were

suggestive of senescence, were observed in various types of endothelial cells including microvascular endothelial cells (Supplementary Figure 1). The same senescence-like changes also occurred in confluent endothelial cells (Supplementary Figure 2). Thus, constitutive activation of Akt induced a senescence-like phenotype in human endothelial cells irrespective of the cell type and growth pattern. To further explore the relationship between Akt activity and cell growth, we isolated clones from AktCA-infected endothelial cells and determined the phospho-Akt level and the cell number on day 30. Clones obtained from mock-infected cell populations could be expanded up to $1-3 \times 10^6$ cells on average and revealed little Akt activity (Figure 1E, lane 1). In contrast, most of the AktCA-infected clones showed almost complete growth arrest and high levels of phospho-Akt expression (Figure 1E, lanes 5-7). However, some AktCA-infected clones showed low phospho-Akt levels and continued to proliferate (Figure 1E, lanes 2-4). Such proliferating populations may lead to underestimation of the growth inhibitory effect of AktCA in long-term culture experiments. The level of phospho-Akt was inversely correlated with the number of cells on day 30 (Figure 1E, right graph). Thus, we concluded that Akt is a negative regulator of the lifespan of primary cultured human endothelial cells.

Upregulation of p21 is essential for Akt-induced growth arrest

To clarify the mechanism of cell growth arrest induced by activation of Akt, we examined the expression of cell cycle regulatory proteins. Expression of p53 and p21^{Waf1/Cip1}, but not p16^{Ink4a}, was elevated, while the level of phosphorylated Rb was decreased in AktCA-infected cells compared with mock-infected cells (Figure 2A), suggesting that Akt may induce growth arrest by upregulating p53 and p21. To determine the role of p21 in Akt-induced cell growth arrest, we infected primary cultured mouse embryonic fibroblasts (MEF) derived from p21-deficient or wild-type mice with AktCA. Similar to endothelial cells, the growth of wild-type MEF was markedly reduced by activation of Akt compared with mock infection (Figure 2B, p21^{+/+}). In contrast, Akt-induced cell growth arrest was restored in p21-deficient MEF (Figure 2B, p21^{-/-}), suggesting that p21 is essential for Akt-induced growth arrest of these cells. It has been reported that expression of p21 is regulated by p53-dependent or -independent transcriptional mechanisms (el-Deiry *et al.*, 1993) as well as protein degradation (Maki and Howley, 1997). To investigate the mechanism by which Akt activation increases p21 expression, we assessed the stability of p21 protein and the extent of p21 transcription. The half-life of p21 protein did not differ between mock- and AktCA-infected endothelial cells (Figure 2C). Northern blot analysis revealed that the level of p21 mRNA was significantly increased in Akt-infected cells compared with mock-infected cells (Figure 2D). Activation of Akt enhanced transcription of the luciferase reporter gene controlled by the promoter fragment of the human p21 gene (Figure 2E), indicating that activation of Akt caused the transcriptional upregulation of p21 expression.

Critical role of p53 transcriptional activity in Akt-induced growth arrest

To ascertain whether Akt activation induces the transcriptional activity of p53, we transfected Akt-infected endothelial

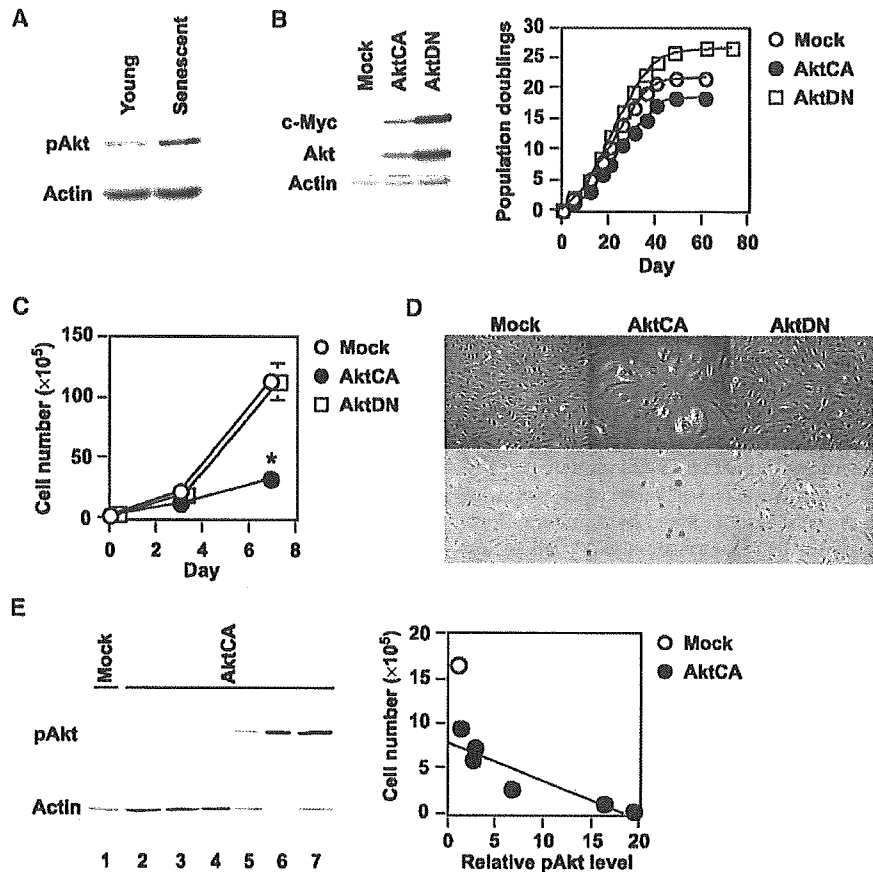


Figure 1 Akt negatively regulates the lifespan of primary cultured human endothelial cells. (A) Whole-cell lysates (30 μ g) of young (passage 4) or senescent (passages 14–15) human endothelial cells were analyzed for the expression of phospho-Akt (pAkt, Ser473) and actin (loading control) by Western blotting. (B) Human endothelial cells were infected with pLNCX (Mock), AktCA or AktDN. After purification, infected cell populations were passaged until they underwent senescence, and the number of cumulative population doublings was determined. Similar results were obtained from three independent experiments. To validate the transduction of AktCA and AktDN, whole-cell lysates (30 μ g) of each infected population were examined for the expression of exogenous myc-tagged Akt (c-Myc) and total Akt (Akt). (C) Human endothelial cells infected with pLNCX (Mock), AktCA or AktDN were purified with G418 for 7 days and seeded at a density of 3×10^5 cells per 100 mm plate on day 0. Cell number per 100 mm plate was then counted at indicated time points. * $P < 0.001$ versus Mock, ANOVA, $n = 4$. (D) Cell morphology (upper panel) and senescence-associated β -galactosidase staining (lower panel) in endothelial cells infected with pLNCX (Mock), AktCA or AktDN. (E) Independent clones were isolated from pLNCX (Mock)- or AktCA-infected endothelial cells. At 30 days after isolation, the cell number of each clone was counted. Whole-cell lysates ($\sim 10 \mu$ g) of isolated clones were also prepared and analyzed for the expression of phospho-Akt by Western blotting (left panel, mock-infected clone for lane 1 and AktCA-infected clones for lanes 2–7). The cell number of each clone was as follows: 16.6×10^5 for lane 1; $6\text{--}10 \times 10^5$ for lanes 2–4; $0.1\text{--}2 \times 10^5$ for lanes 5–7. As the availability of samples was limited in the case of most AktCA-infected clones, the lysates used were less than 10 μ g (lanes 5–7). Therefore, the levels of phospho-Akt were standardized on the basis of actin expression, and the relative level of phospho-Akt and the cell number of each clone were plotted in the graph (right panel, $r = 0.92$, $P < 0.01$). The corrected value of phospho-Akt in mock-infected clones (lane 1) is set at 1.

cells with the luciferase reporter gene containing 13 copies of the p53-binding consensus sequence (PG13). Introduction of AktCA induced p53 promoter-driven luciferase activity compared with mock infection, but not luciferase activity driven by a promoter containing 15 copies of a similar sequence with mutation at critical positions (MG15) (Figure 3A). To further assess the relation between Akt and p53 transcription activity, we tested whether ablation of p53 could circumvent Akt-induced growth arrest. We infected human endothelial cells with a retroviral vector encoding the E6 oncoprotein of HPV16, which binds p53 and facilitates its destruction by ubiquitin-mediated proteolysis (pBabe E6). We also infected the same cells with the empty vector encoding resistance to puromycin alone (pBabe). Both cell populations were then

subjected to infection with pLNCX or AktCA. Activation of Akt markedly inhibited the growth of pBabe-infected endothelial cells (Figure 3B, pBabe), while growth inhibition was completely abolished in E6-infected cells (Figure 3B, E6). Changes of cell morphology were also reversed to normal by introduction of E6 (Figure 3C). Ablation of p53 also lessened the decrease in the lifespan of AktCA-infected cells (Supplementary Figure 3). These results indicate a critical role of p53 in Akt-induced cell growth arrest. Introduction of AktCA did not induce p21 expression in E6-infected cells (Figure 3D), suggesting that constitutive activation of Akt increases induction of the transcription of p21 by a p53-dependent mechanism and thereby promotes cell growth arrest.

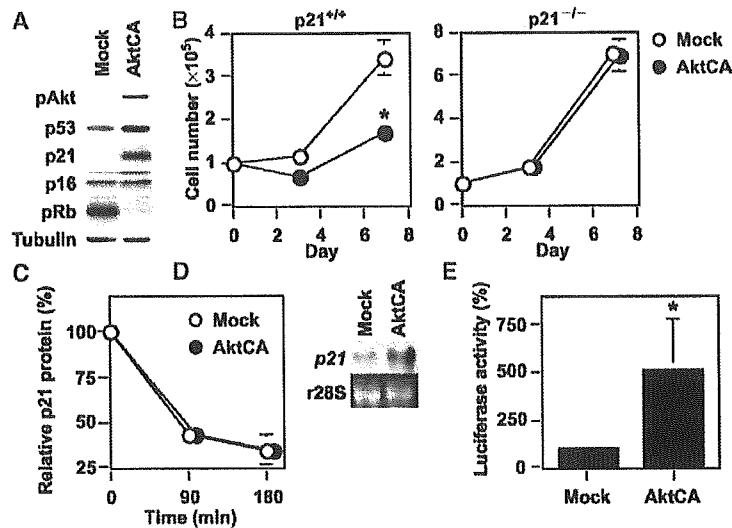


Figure 2 Upregulation of p21 is essential for Akt-induced growth arrest. (A) Whole-cell lysates (30 μ g) of pLNCX (Mock)- or AktCA-infected endothelial cells on day 0 were examined for the expression of phospho-Akt (pAkt), cell cycle regulatory proteins and tubulin (loading control) by Western blotting. (B) MEF derived from wild-type ($p21^{+/+}$) or $p21$ -deficient mice ($p21^{-/-}$) were infected with pLNCX (Mock) or AktCA, purified with G418 for 7 days and seeded at a density of 1×10^5 cells per 100 mm plate on day 0. Cell number per 100 mm plate was then counted at indicated time points. * $P < 0.001$ versus Mock, ANOVA, $n = 4$. (C) Human endothelial cells infected with pLNCX (Mock) or AktCA were treated with cycloheximide (10 μ g/ml) for the indicated time interval. Whole-cell lysates (30 μ g) were then prepared at each time point and assayed for the expression of p21 and actin (loading control) by Western blotting. The graph indicates the results of densitometric analysis for the levels of p21 protein relative to actin expression. The value at time 0 is set at 100%. (D) Total RNA (30 μ g) was extracted from human endothelial cells infected with pLNCX (Mock) or AktCA and analyzed for $p21$ mRNA levels by Northern blotting (upper panel). Ribosomal RNA was used as an internal control (lower panel). (E) The luciferase reporter gene plasmid controlled by the promoter of the human $p21$ gene was transfected into endothelial cells infected with pLNCX (Mock) or AktCA 24 h before the luciferase activity was measured. The activity in mock-infected cells is set at 100%. * $P < 0.05$ versus Mock, paired t -test, $n = 4$.

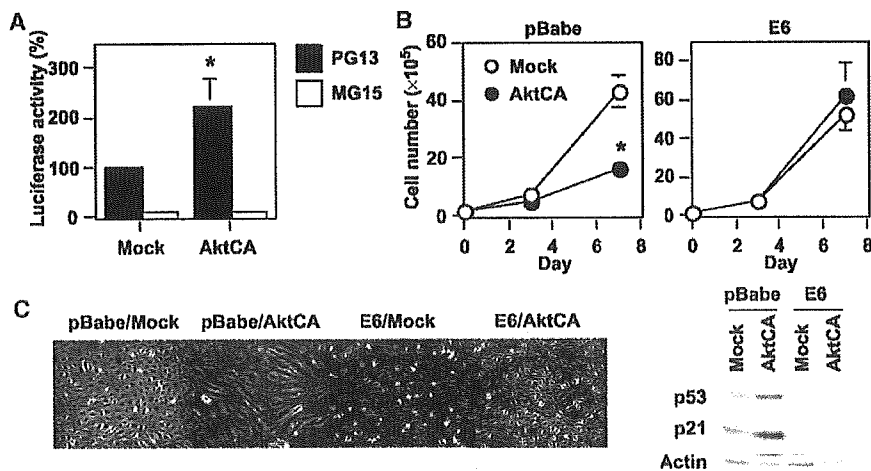


Figure 3 Critical role of p53 transcriptional activity in Akt-induced growth arrest. (A) The luciferase reporter gene plasmid pPG13-Luc containing the p53-binding sequence or pMG15-Luc containing the mutated p53-binding sequence was transfected into endothelial cells infected with pLNCX (Mock) or AktCA 24 h before the luciferase activity was measured. The activity of PG13-Luc in mock-infected cells is set at 100%. * $P < 0.005$ versus Mock, ANOVA, $n = 4$. (B) Human endothelial cells were infected with pBabe (empty vector) or pBabe E6 and purified with puromycin. Infected cells were then transduced with pLNCX or AktCA as described in Figure 1C and seeded at a density of 2×10^5 cells per 100 mm plate on day 0. Cell number was then counted at indicated time points. * $P < 0.05$ versus Mock, ANOVA, $n = 4$. (C) Morphology of cell populations prepared in (B). (D) Whole-cell lysates (30 μ g) were extracted from cells prepared in (B) and examined for the expression of p53, p21 and actin (loading control).

Forkhead transcription factor mediates Akt-induced growth arrest

In *C. elegans*, a reduction-of-function mutation in the PI3K/Akt pathway leads to activation of the forkhead transcription factor

DAF-16, resulting in extension of the lifespan, and this effect is inhibited by mutations of antioxidant genes (Murphy *et al*, 2003). Recent evidence indicates that the mammalian forkhead transcription factor FOXO3a (also known as FKHR-L1)

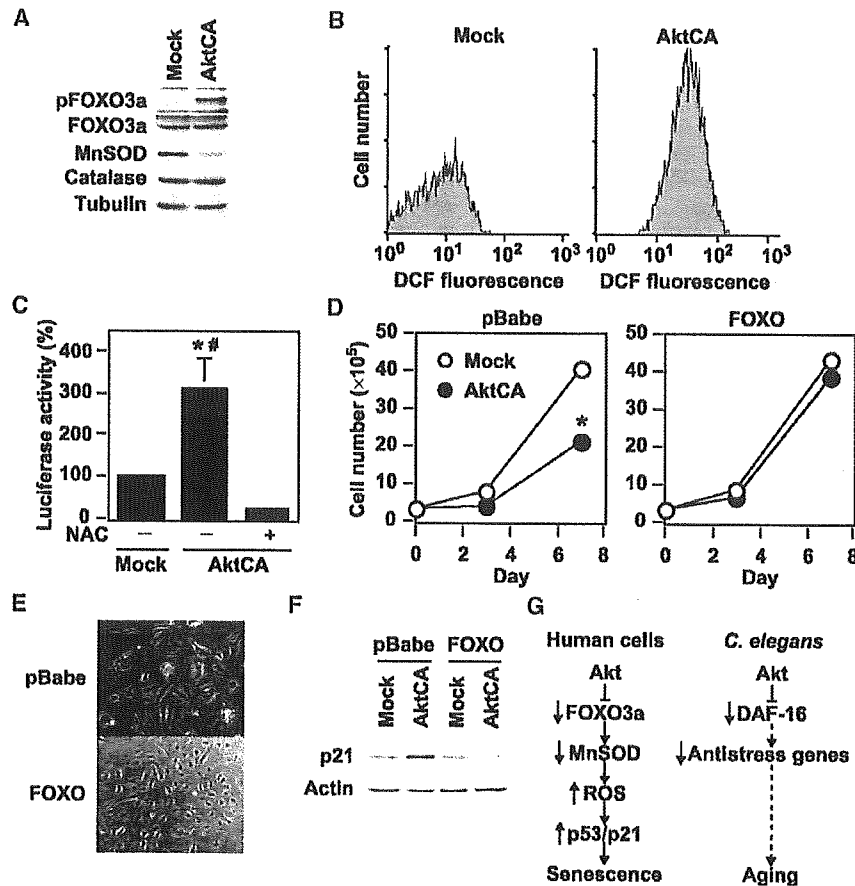


Figure 4 FOXO3a mediates Akt-induced growth arrest via the ROS/p53/p21-dependent mechanisms. (A) Whole-cell lysates (30 μ g) of pLNCX (Mock)- or AktCA-infected endothelial cells were examined for expression of phospho-FOXO3a (pFOXO3a, Thr32), total FOXO3a (FOXO3a), MnSOD, catalase and tubulin (loading control) by Western blotting. (B) Human endothelial cells infected with pLNCX (Mock) or AktCA were loaded with DCF for 30 min and analyzed by FACS. Representative results from two independent experiments are shown. (C) The luciferase reporter gene plasmid PG13-Luc was transfected into endothelial cells infected with pLNCX (Mock) or AktCA and cultured in the absence or presence of NAC (0.5 mM). At 24 h after transfection, the luciferase activity was measured. The activity in mock-infected cells is set at 100%. * $P < 0.01$ versus Mock, # $P < 0.001$ versus AktCA + NAC, ANOVA, $n = 4$. (D) Human endothelial cells were infected with pBabe (empty vector) or pBabe mutant FOXO3a (FOXO). Infected cell populations were then transduced with pLNCX (Mock) or AktCA and seeded at a density of 3×10^5 cells per 100 mm plate on day 0. Cell number was then counted at indicated time points. * $P < 0.05$ versus Mock, ANOVA, $n = 3$. (E) Morphology of Akt-infected cell populations prepared in (D). (F) Whole-cell lysates (30 μ g) prepared in (D) were examined for the expression of p21 and actin (loading control) by Western blotting. Constitutive activation of Akt inhibits the transcriptional activity of FOXO3a and thereby downregulates *MnSOD*, leading to an increase of ROS that promotes senescence-like growth arrest via the p53/p21-dependent pathway. (G) Proposed signaling pathway of Akt-induced senescence in human endothelial cells compared with that in *C. elegans*. Akt inactivates FOXO3a and thereby downregulates its target antioxidant gene *MnSOD*, leading to an increase of ROS. ROS induces p53 activity, resulting in upregulation of p21 expression, which promotes cellular senescence in human endothelial cells. In *C. elegans*, the PI3K/Akt pathway also negatively regulates longevity by inactivating DAF-16 activity. This regulatory pathway partly involves the decreased expression of anti-stress genes including *SOD*.

upregulates radical scavenger genes that have a protective effect against oxidative damage in human cells (Kops *et al*, 2002; Nemoto and Finkel, 2002). To investigate the role of FOXO3a in Akt-induced growth arrest, we examined the expression of FOXO3a and antioxidant genes. Phosphorylated FOXO3a (the inactive form) was increased in AktCA-infected endothelial cells compared with mock-infected cells (Figure 4A). The level of manganese superoxide dismutase (MnSOD), but not catalase, was reduced in AktCA-infected endothelial cells (Figure 4A). Consistent with the decreased level of MnSOD, AktCA-infected endothelial cells exhibited an increase of reactive oxygen species (ROS), as assessed using the redox-sensitive fluorophore 2',7'-dichlorofluorescein diace-

tate (DCF) (Figure 4B). Since oxidative stress is postulated to induce the activation of p53 (Finkel and Holbrook, 2000), we examined the effect of an ROS scavenger, *N*-acetyl cysteine (NAC), on p53 promoter activity (PG13) in AktCA-infected endothelial cells. The enhancement of p53 promoter-driven luciferase activity by AktCA was significantly lessened after treatment with NAC, suggesting that ROS are involved in Akt-induced senescence-like growth arrest (Figure 4C). To further determine the causal link between Akt-induced growth arrest and phosphorylation of FOXO3a, we tested a mutated FOXO3a that was resistant to phosphorylation by Akt. Introduction of this FOXO3a mutant prevented senescence-like growth arrest and cellular morphological changes induced by activation of

Akt (Figures 4D and E). Moreover, induction of p21 expression by Akt activation was effectively inhibited by the mutant form of FOXO3a (Figure 4F). These results suggest that constitutive activation of Akt inhibits the transcriptional activity of FOXO3a and thereby downregulates *MnSOD*, leading to an increase of ROS that promotes senescence-like growth arrest via the p53/p21-dependent pathway (Figure 4G). This signaling pathway could be recaptured in endothelial cells undergoing replicative senescence (Supplementary Figure 4), which suggests that Akt-induced growth arrest is relevant to physiological senescence and may also be involved in human vasculopathy.

Pathophysiological role of Akt-induced endothelial cell senescence

To investigate whether atherogenic stimuli could activate Akt in human atheroma tissues, we examined Akt activity in coronary arteries obtained at autopsy from patients who had ischemic heart disease. We detected Akt activity in endothelial cells on the surface of coronary atherosclerotic lesions, but not in those of the internal mammary arteries from the same patients, which showed minimal atherosclerotic changes (Figure 5A). To investigate the potential role of Akt-induced endothelial senescence in the pathogenesis of vasculopathy, we examined the effect of Akt on angiogenic activity and the expression of proinflammatory molecules. Tube formation by AktCA-infected endothelial cells was significantly reduced compared with that by mock-infected cells (Figure 5B). In addition, expression of intercellular adhesion molecule (ICAM)-1 was increased in AktCA-infected endothelial cells (Figure 5C). To further explore the role of Akt-induced senescence, we tested the influence of insulin on endothelial cell senescence. Treatment with insulin at a pathological dose caused increases in phospho-FOXO3a and p53 activity (Figures 6A and B), which were comparable to the changes seen in AktCA-infected cells. This increase was inhibited by introduction of AktDN (data not shown), indicating that it was dependent on Akt activity. Insulin induced p53 activity in a dose-dependent manner (Figure 6B). Moreover, continuous incubation with insulin was found to accelerate senescence of human endothelial cells, and this effect was also dose dependent (Figure 6C). Thus, it is conceivable that constitutive activation of Akt by growth factors may promote endothelial cell senescence and thereby contribute to vascular pathophysiology.

Discussion

Our results suggested a critical role of Akt activation in regulating the lifespan of primary cultured human cells in a manner similar to the control of longevity by the PI3K/Akt

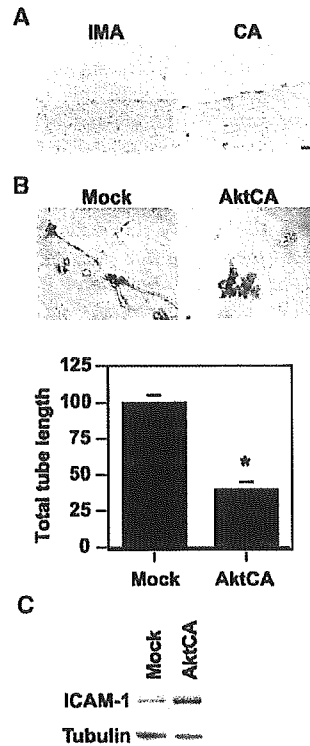


Figure 5 Pathophysiological role of Akt-induced endothelial cell senescence. (A) Immunohistochemistry for phospho-Akt (brown) in the coronary arteries (CA) and the internal mammary arteries (IMA) from the same patients. Scale bar: 10 μ m. (B) Tube formation assay. Human endothelial cells infected with pLNCX (Mock) or AktCA were seeded onto Matrigel. After 48 h, the total tube length was estimated by an angiogenesis image analyzer (Kurabo, Osaka, Japan). The graph shows relative tube length in Mock- and AktCA-infected cells. The length in Mock-infected cells is set at 100%. * $P < 0.005$ versus Mock, unpaired *t*-test, $n = 4$. (C) Whole-cell lysates (30 μ g) of pLNCX (Mock)- or AktCA-infected endothelial cells were examined for the expression of ICAM-1 and tubulin (loading control) by Western blotting.

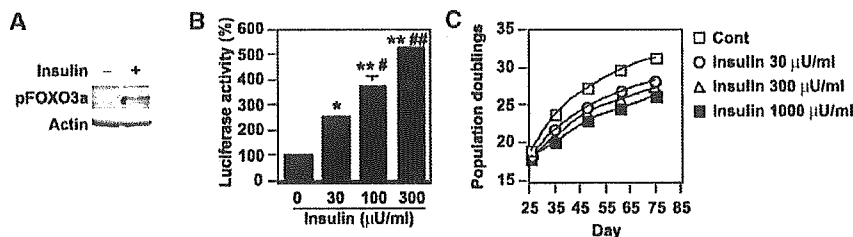


Figure 6 Insulin promotes endothelial cell senescence. (A) Whole-cell lysates (30 μ g) of human endothelial cells treated with insulin (1000 μ U/ml) for 30 min were analyzed for the levels of phosphorylated FOXO3a and actin (loading control) by Western blotting. (B) The luciferase reporter gene plasmid PG13-Luc was transfected into endothelial cells in the presence of insulin at the indicated dose. At 24 h after transfection, the luciferase activity was measured. The activity in controls is set at 100%. * $P < 0.05$, ** $P < 0.0001$ versus control, # $P < 0.01$, ### $P < 0.001$ versus insulin 30 μ U/ml, $n = 4$. (C) Human endothelial cells were cultured in the presence of insulin at the indicated dose and passaged. The number of cumulative population doublings was determined ($n = 3$).

signaling pathway in *C. elegans*. We have previously demonstrated that senescent endothelial cells are present in human atherosclerotic plaques, but not nonatherosclerotic lesions, and express high levels of proinflammatory molecules that are known to promote atherogenesis (Minamino *et al*, 2002). Since Akt is known to be activated by various atherogenic stimuli (Cantley, 2002), our findings imply that constitutive activation of Akt by atherogenic stimuli may induce endothelial cell senescence in atheroma tissue and thereby contribute to atherogenesis. Consistent with this hypothesis, we observed that Akt was phosphorylated in human atheroma but not in normal arteries, and that expression of proinflammatory molecules was increased in AktCA-infected endothelial cells compared with mock-infected cells. Moreover, insulin increased p53 activity via an Akt-dependent mechanism and reduced the lifespan of endothelial cells. Thus, an Akt-induced senescence-like phenotype may be particularly involved in diabetic vasculopathy, since hyperinsulinemia could constitutively activate Akt in endothelial cells.

Although one supposes that Akt-induced senescence might be an artifact, the following points suggest that our findings are valid. First, we observed that Akt activity was increased in endothelial cells undergoing replicative senescence and that inhibition of this endogenous increase in Akt activity by AktDN led to prolongation of the cellular lifespan. This is compatible with many earlier studies demonstrating that reduction-of-function mutations in the insulin/PI3K/Akt pathway extend longevity in organisms ranging from yeast to mice (Longo and Finch, 2003). This signaling pathway (including phosphorylation of FOXO3a and downregulation of MnSOD induced by Akt) could be recaptured in endothelial cells undergoing replicative senescence (Supplementary Figure 4), which suggests that Akt-induced growth arrest may be relevant to physiological senescence. Second, we found that growth was significantly decreased in cloned populations obtained from cells infected with AktCA that exhibited a moderate increase in Akt activity (Figure 1, lanes 2–4). The level of Akt activity in these cells was similar to that in endothelial cells undergoing replicative senescence, suggesting that a physiological level of Akt activation may be able to promote cellular senescence. Third, we found that phospho-FOXO3a levels in AktCA-infected cells were comparable to those in endothelial cells stimulated by insulin at the level seen in patients with type II diabetes. The p53 transcriptional activity in AktCA-infected cells was also similar to that of cells treated with insulin. These results indicate that the pathophysiological activation of Akt was mimicked by infection with AktCA.

Gain-of-function mutations in the PI3K/Akt signaling pathway are frequently found in human cancers (Testa and Bellacosa, 2001). Thus, Akt-induced growth arrest may be another antitumorigenesis mechanism similar to Ras-induced senescence (Serrano *et al*, 1997; Campisi, 2001; Wright and Shay, 2001). We found that ablation of p53 prevented Akt-induced growth arrest, whereas both the p53- and p16-dependent pathways are reported to be essential for Ras-induced senescence (Serrano *et al*, 1997; Lin *et al*, 1998). Oncogenic Ras also induced premature senescence of primary cultured human vascular cells, which was suppressed by inhibition of mitogen-activated protein kinase but not PI3K (Minamino *et al*, 2003), suggesting that Akt-induced growth arrest may be distinct from Ras-induced senescence.

A recent study demonstrated that senescent cells could potentiate the oncogenic transformation of nearby normal cells (Krtolica *et al*, 2001), which suggests that induction of senescence by Akt as well as Ras may actually be pro-oncogenic.

We found that Akt increased the transcriptional activity of p53, resulting in upregulation of *p21* in primary cultured human endothelial cells. Our results are consistent with previous reports that Akt mediates induction of *p21* expression by various stimuli in myoblasts and vascular cells (Lawlor and Rotwein, 2000a,b; Schonherr *et al*, 2001). However, Akt is also reported to induce cytoplasmic localization of *p21* (Zhou *et al*, 2001a), thereby promoting cell proliferation, and to promote nuclear translocation of Mdm2 (a negative regulator of p53), leading to a reduction of both p53 levels and transactivation (Mayo and Donner, 2001; Zhou *et al*, 2001b). Such changes were not observed in human endothelial cells (H Miyauchi, unpublished data). It is noteworthy that most other studies have examined immortal cells, in which the normal cell cycle machinery might be impaired, and the effects of constitutive Akt activation have not been explored. Although the effects of tissue-specific transgenic expression of constitutively activated *Akt* alleles have been reported in several different murine models, most of these animals do not develop tumors (Vivanco and Sawyers, 2002), suggesting that activation of Akt is insufficient to cause cancer unless combined with other oncogenic stimuli. Thus, like Ras, Akt may promote cell proliferation and survival or senescence-like growth arrest, depending on various factors including the cellular context as well as the duration and extent of its activation.

In conclusion, we found that Akt negatively regulates the lifespan of primary cultured human endothelial cells via the p53/p21-dependent pathway, and this action is mediated at least partly by the forkhead transcription factor that regulates cellular ROS levels. Our data not only support the previous findings about the signaling pathway for longevity in *C. elegans*, but also provide a novel insight for research on the treatments of human vasculopathy and cancer.

Materials and methods

Cell culture

Human aortic endothelial cells, human dermal microvascular endothelial cells and human umbilical vein endothelial cells were purchased from Bio Whittaker (Walkersville, MD), and cultured according to the manufacturer's instructions. These cells gave similar results (data not shown). We defined senescent cells as the cultures that do not increase in the cell number and remain subconfluent for 2 weeks. We confirmed the senescent phenotype with SA- β -gal activity assay. Wild-type and *p21*-deficient MEFs were prepared from day 13.5 embryos derived from crosses between *p21*^{-/-} mice (Jackson, Bar Harbor, ME) and cultured in DMEM plus 10% fetal bovine serum. Senescence-associated β -galactosidase staining was performed as described (Minamino *et al*, 2002). Tube formation assay was performed according to the manufacturer's instructions (BioCoat Angiogenesis System, Clontech, Palo Alto, CA).

Retroviral infection

The following plasmids were used for generating retroviruses: pLNCX (Clontech, Palo Alto, CA) and pBabe (a gift from Dr CW Lowe, Cold Spring Harbor Laboratory, Cold Spring Harbor, NY). We created the pLNCX-based vector expressing a constitutively active form of Akt (AktCA) or a dominant-negative form of Akt (AktDN) by using the fragment derived from the plasmid pBS-CA-Akt or

pBS-DN-Akt (Fujishiro *et al*, 2001), respectively (a gift from Dr T Asano, Tokyo University, Tokyo, Japan). The pBabe-based vector expressing a mutant form of FOXO3a was constructed by using the fragment derived from pECE FOXO3aTM (Brunet *et al*, 1999) (a gift from Dr ME Greenberg, Harvard Medical School, Boston, MA). We also constructed the pBabe-based vector expressing E6 (pBabe E6). Details of the construct are available upon request. Retroviral stocks were generated by transient transfection of packaging cell line (PT67, Clontech) and stored at -80°C until use. Human endothelial cells (passage 4–6) were plated at 5×10^5 cells per 100-mm-diameter dish 24 h before infections. For infections, the culture medium was replaced by retroviral stocks supplemented with 8 $\mu\text{g}/\text{ml}$ polybrene (Sigma, Tokyo, Japan). At 48 h after infections, the infected cell populations were selected by culture in 500 $\mu\text{g}/\text{ml}$ G418 for 7 days (pLNCX-based vectors). After selection, $1\text{--}3 \times 10^5$ cells were seeded onto 100-mm-diameter dishes on the 8th day postinfection. The 8th day after infection is designated as day 0. For double infection, endothelial cells were infected with pBabe, pBabe FOXO3a or pBabe E6 purified with 0.8 $\mu\text{g}/\text{ml}$ puromycin for 4 days and subjected to the second infection as described above.

Western blotting and antibodies

Whole-cell lysates (30 μg) were resolved by SDS polyacrylamide gel electrophoresis (PAGE). Proteins were transferred onto a polyvinylidene difluoride (PVDF) membrane (Millipore, Bedford, MA) and incubated with the first antibody followed by an anti-rabbit immunoglobulin G-horseradish peroxidase antibody or anti-mouse immunoglobulin G-horseradish peroxidase antibody (Jackson, West Grove, PA). Specific proteins were detected using enhanced chemiluminescence (Amersham, Tokyo, Japan). The first antibodies used for Western blotting are as follows: antibodies to Akt, p53, ICAM-1, actin and tubulin (Santa Cruz, Santa Cruz, CA); antibodies to retinoblastoma protein and p16 (Pharmingen, Tokyo, Japan); anti-p21 antibody (Oncogene, Cambridge, MA); anti-phospho-Akt (Ser473) antibody (Cell Signaling, Beverly, MA); anti-catalase antibody (Sigma); antibodies to FOXO3a, phospho-FOXO3a (Thr32) and MnsOD (Upstate Biotechnology, Lake Placid, NY).

Northern blotting

Total RNA (30 μg) was extracted using RNAzol B (Tel Test, Friendswood, TX) according to the manufacturer's instructions, separated on a formaldehyde denaturing gel and transferred to a nylon membrane (Amersham). The blot was then hybridized with radiolabeled p21 cDNA probes using the Quickhyb hybridization solution (Stratagene, Tokyo, Japan) according to the manufacturer's instructions.

References

- Blüher M, Kahn BB, Kahn CR (2003) Extended longevity in mice lacking the insulin receptor in adipose tissue. *Science* **299**: 572–574
- Blume-Jensen P, Hunter T (2001) Oncogenic kinase signalling. *Nature* **411**: 355–365
- Brunet A, Bonni A, Zigmond MJ, Lin MZ, Juo P, Hu LS, Anderson MJ, Arden KC, Blenis J, Greenberg ME (1999) Akt promotes cell survival by phosphorylating and inhibiting a Forkhead transcription factor. *Cell* **96**: 857–868
- Campisi J (2001) Cellular senescence as a tumor-suppressor mechanism. *Trends Cell Biol* **11**: S27–S31
- Cantley LC (2002) The phosphoinositide 3-kinase pathway. *Science* **296**: 1655–1657
- Cardone MH, Roy N, Stennicke HR, Salvesen GS, Franke TF, Stanbridge E, Frisch S, Reed JC (1998) Regulation of cell death protease caspase-9 by phosphorylation. *Science* **282**: 1318–1321
- Cheng JQ, Altomare DA, Klein MA, Lee WC, Kruh GD, Lissy NA, Testa JR (1997) Transforming activity and mitosis-related expression of the AKT2 oncogene: evidence suggesting a link between cell cycle regulation and oncogenesis. *Oncogene* **14**: 2793–2801
- Cheng JQ, Ruggeri B, Klein WM, Sonoda G, Altomare DA, Watson DK, Testa JR (1996) Amplification of AKT2 in human pancreatic cells and inhibition of AKT2 expression and tumorigenicity by antisense RNA. *Proc Natl Acad Sci USA* **93**: 3636–3641

Luciferase assays

The reporter gene plasmid (1 μg) was transfected into endothelial cells infected with pLNCX (Mock) or AktCA 24 h before luciferase assay. The control vector encoding *Renilla* luciferase (0.1 μg) was co-transfected for an internal control. Luciferase assay was carried out using a dual-luciferase reporter assay system (Promega, Madison, WI) according to the manufacturer's instructions. The plasmids pPG13-Luc, pPG15-Luc and pWWP-LUC-1 (el-Deiry *et al*, 1993) were a gift from Dr B Vogelstein (Johns Hopkins University, Baltimore, MD).

Tissue specimens and histology

Human coronary arteries and internal mammary arteries were obtained from four autopsied individuals who had ischemic heart disease. For immunohistochemistry, the frozen sections (6 μm) were treated with 0.3% hydrogen peroxide in methanol for 20 min, preincubated with 5% goat serum and then treated with anti-phospho-Akt antibody (1:100; Santa Cruz, Santa Cruz, CA) for 1 h at 37°C . Next, the sections were incubated with a biotinylated goat secondary antibody, treated with the avidin-biotin complex (Elite ABC kit, Vector, Burlingame, CA) and stained with diaminobenzidine tetrahydrochloride and hydrogen peroxide. To verify the specificity of the first antibodies, we performed a control staining with nonimmune IgG and excluded the possibility of nonspecific signals. The studies on human samples were approved by our institutional review board.

Statistical analysis

All values were expressed as mean \pm s.e.m. Comparison of results between different groups was performed by one-way analysis of variance, paired *t*-test and unpaired *t*-test using StatView 4.5 (Abacus Concepts, Berkeley, CA).

Supplementary data

Supplementary data are available at *The EMBO Journal* Online.

Acknowledgements

We thank Dr B Vogelstein, SW Lowe, ME Greenberg and T Asano for reagents. This work was supported by grants from Takeda Medical Research Foundation, Takeda Science Foundation, Japan Heart Foundation, Mochida Memorial Foundation, Uehara Memorial Foundation, Mitsubishi Pharma Research Foundation and the Ministry of Education, Science, Sports, and Culture of Japan (to TM and IK).

Competing interests statement

The authors declare that they have no competing financial interests.

- Faragher RG, Kipling D (1998) How might replicative senescence contribute to human ageing? *BioEssays* **20**: 985-991
- Finkel T, Holbrook NJ (2000) Oxidants, oxidative stress and the biology of ageing. *Nature* **408**: 239-247
- Fujishiro M, Gotoh Y, Katagiri H, Sakoda H, Ogihara T, Anai M, Onishi Y, Ono H, Funaki M, Inukai K, Fukushima Y, Kikuchi M, Oka Y, Asano T (2001) MKK6/3 and p38 MAPK pathway activation is not necessary for insulin-induced glucose uptake but regulates glucose transporter expression. *J Biol Chem* **276**: 19800-19806
- Guarente L, Kenyon C (2000) Genetic pathways that regulate ageing in model organisms. *Nature* **408**: 255-262
- Hayflick L (1975) Current theories of biological aging. *Fed Proc* **34**: 9-13
- Holzenberger M, Dupont J, Ducus B, Leneuve P, Geloën A, Even PC, Cervera P, Le Bouc Y (2003) IGF-1 receptor regulates lifespan and resistance to oxidative stress in mice. *Nature* **421**: 182-187
- Honda Y, Honda S (1999) The daf-2 gene network for longevity regulates oxidative stress resistance and Mn-superoxide dismutase gene expression in *Caenorhabditis elegans*. *FASEB J* **13**: 1385-1393
- Kenyon C (2001) A conserved regulatory system for aging. *Cell* **105**: 165-168
- Kenyon C, Chang J, Gensch E, Rudner A, Tabtiang R (1993) A *C. elegans* mutant that lives twice as long as wild type. *Nature* **366**: 461-464
- Kops GJ, Dansen TB, Polderman PE, Saarloos I, Wirtz KW, Coffey PJ, Huang TT, Bos JL, Medema RH, Burgering BM (2002) Forkhead transcription factor FOXO3a protects quiescent cells from oxidative stress. *Nature* **419**: 316-321
- Krtolica A, Parrinello S, Lockett S, Desprez PY, Campisi J (2001) Senescent fibroblasts promote epithelial cell growth and tumorigenesis: a link between cancer and aging. *Proc Natl Acad Sci USA* **98**: 12072-12077
- Lawlor MA, Rotwein P (2000a) Coordinate control of muscle cell survival by distinct insulin-like growth factor activated signaling pathways. *J Cell Biol* **151**: 1131-1140
- Lawlor MA, Rotwein P (2000b) Insulin-like growth factor-mediated muscle cell survival: central roles for Akt and cyclin-dependent kinase inhibitor p21. *Mol Cell Biol* **20**: 8983-8995
- Lee RY, Hench J, Ruvkun G (2001) Regulation of *C. elegans* DAF-16 and its human ortholog FOXO3a by the daf-2 insulin-like signaling pathway. *Curr Biol* **11**: 1950-1957
- Lin AW, Barradas M, Stone JC, van Aelst L, Serrano M, Lowe SW (1998) Premature senescence involving p53 and p16 is activated in response to constitutive MEK/MAPK mitogenic signaling. *Genes Dev* **12**: 3008-3019
- Lin K, Dorman JB, Rodan A, Kenyon C (1997) daf-16: An HNF-3/ forkhead family member that can function to double the life-span of *Caenorhabditis elegans*. *Science* **278**: 1319-1322
- Lin K, Hsin H, Libina N, Kenyon C (2001) Regulation of the *Caenorhabditis elegans* longevity protein DAF-16 by insulin/IGF-1 and germline signaling. *Nat Genet* **28**: 139-145
- Longo VD, Finch CE (2003) Evolutionary medicine: from dwarf model systems to healthy centenarians? *Science* **299**: 1342-1346
- Maki CG, Howley PM (1997) Ubiquitination of p53 and p21 is differentially affected by ionizing and UV radiation. *Mol Cell Biol* **17**: 355-363
- Mayo LD, Donner DB (2001) A phosphatidylinositol 3-kinase/Akt pathway promotes translocation of Mdm2 from the cytoplasm to the nucleus. *Proc Natl Acad Sci USA* **98**: 11598-11603
- Medema RH, Kops GJ, Bos JL, Burgering BM (2000) AFX-like Forkhead transcription factors mediate cell-cycle regulation by Ras and PKB through p27kip1. *Nature* **404**: 782-787
- Minamino T, Miyauchi H, Yoshida T, Ishida Y, Yoshida H, Komuro I (2002) Endothelial cell senescence in human atherosclerosis: role of telomere in endothelial dysfunction. *Circulation* **105**: 1541-1544
- Minamino T, Yoshida T, Tateno K, Miyauchi H, Zou Y, Toko H, Komuro I (2003) Ras-induced vascular smooth muscle cell senescence in human atherosclerosis. *Circulation* **108**: 2264-2269
- Morris JZ, Tissenbaum HA, Ruvkun G (1996) A phosphatidylinositol-3-OH kinase family member regulating longevity and diapause in *Caenorhabditis elegans*. *Nature* **382**: 536-539
- Murphy CT, McCarroll SA, Bargmann CI, Fraser A, Kamath RS, Ahringer J, Li H, Kenyon C (2003) Genes that act downstream of DAF-16 to influence the lifespan of *Caenorhabditis elegans*. *Nature* **424**: 277-283
- Nemoto S, Finkel T (2002) Redox regulation of forkhead proteins through a p66shc-dependent signaling pathway. *Science* **295**: 2450-2452
- Ogg S, Paradis S, Gottlieb S, Patterson GI, Lee L, Tissenbaum HA, Ruvkun G (1997) The Fork head transcription factor DAF-16 transduces insulin-like metabolic and longevity signals in *C. elegans*. *Nature* **389**: 994-999
- Paradis S, Ruvkun G (1998) *Caenorhabditis elegans* Akt/PKB transduces insulin receptor-like signals from AGE-1 PI3 kinase to the DAF-16 transcription factor. *Genes Dev* **12**: 2488-2498
- Rohme D (1981) Evidence for a relationship between longevity of mammalian species and life spans of normal fibroblasts *in vitro* and erythrocytes *in vivo*. *Proc Natl Acad Sci USA* **78**: 5009-5013
- Schonherr E, Levkau B, Schaefer L, Kresse H, Walsh K (2001) Decorin-mediated signal transduction in endothelial cells. Involvement of Akt/protein kinase B in up-regulation of p21(WAF1/CIP1) but not p27(KIP1). *J Biol Chem* **276**: 40687-40692
- Serrano M, Lin AW, McCurrach ME, Beach D, Lowe SW (1997) Oncogenic ras provokes premature cell senescence associated with accumulation of p53 and p16INK4a. *Cell* **88**: 593-602
- Shin I, Yakes FM, Rojo F, Shin NY, Bakin AV, Baselga J, Arteaga CL (2002) PKB/Akt mediates cell-cycle progression by phosphorylation of p27(Kip1) at threonine 157 and modulation of its cellular localization. *Nat Med* **8**: 1145-1152
- Tatar M, Kopelman A, Epstein D, Tu MP, Yin CM, Garofalo RS (2001) A mutant *Drosophila* insulin receptor homolog that extends lifespan and impairs neuroendocrine function. *Science* **292**: 107-110
- Testa JR, Bellacosa A (2001) AKT plays a central role in tumorigenesis. *Proc Natl Acad Sci USA* **98**: 10983-10985
- Thompson KV, Holliday R (1983) Genetic effects on the longevity of cultured human fibroblasts. II. DNA repair deficient syndromes. *Gerontology* **29**: 83-88
- Viglietto G, Motti ML, Bruni P, Melillo RM, D'Alessio A, Califano D, Vinci F, Chiappetta G, Tschlis P, Bellacosa A, Fusco A, Santoro M (2002) Cytoplasmic relocalization and inhibition of the cyclin-dependent kinase inhibitor p27(Kip1) by PKB/Akt-mediated phosphorylation in breast cancer. *Nat Med* **8**: 1136-1144
- Vivanco I, Sawyers CL (2002) The phosphatidylinositol 3-Kinase AKT pathway in human cancer. *Nat Rev Cancer* **2**: 489-501
- Weinstein BS, Ciszek D (2002) The reserve-capacity hypothesis: evolutionary origins and modern implications of the trade-off between tumor-suppression and tissue-repair. *Exp Gerontol* **37**: 615-627
- Wright WE, Shay JW (2001) Cellular senescence as a tumor-protection mechanism: the essential role of counting. *Curr Opin Genet Dev* **11**: 98-103
- Zhou BP, Liao Y, Xia W, Spohn B, Lee MH, Hung MC (2001a) Cytoplasmic localization of p21Cip1/WAF1 by Akt-induced phosphorylation in HER-2/neu-overexpressing cells. *Nat Cell Biol* **3**: 245-252
- Zhou BP, Liao Y, Xia W, Zou Y, Spohn B, Hung MC (2001b) HER-2/neu induces p53 ubiquitination via Akt-mediated MDM2 phosphorylation. *Nat Cell Biol* **3**: 973-982

Salt-sensitive hypertension is triggered by Ca^{2+} entry via $\text{Na}^+/\text{Ca}^{2+}$ exchanger type-1 in vascular smooth muscleTakahiro Iwamoto^{1,3}, Satomi Kita^{1,5}, Jin Zhang², Mordecai P Blaustein², Yuji Arai⁴, Shigeru Yoshida⁵, Koji Wakimoto⁶, Issei Komuro⁷ & Takeshi Katsuragi¹

Excessive salt intake is a major risk factor for hypertension. Here we identify the role of $\text{Na}^+/\text{Ca}^{2+}$ exchanger type 1 (NCX1) in salt-sensitive hypertension using SEA0400, a specific inhibitor of Ca^{2+} entry through NCX1, and genetically engineered mice. SEA0400 lowers arterial blood pressure in salt-dependent hypertensive rat models, but not in other types of hypertensive rats or in normotensive rats. Infusion of SEA0400 into the femoral artery in salt-dependent hypertensive rats increases arterial blood flow, indicating peripheral vasodilation. SEA0400 reverses ouabain-induced cytosolic Ca^{2+} elevation and vasoconstriction in arteries. Furthermore, heterozygous NCX1-deficient mice have low salt sensitivity, whereas transgenic mice that specifically express NCX1.3 in smooth muscle are hypersensitive to salt. SEA0400 lowers the blood pressure in salt-dependent hypertensive mice expressing NCX1.3, but not in SEA0400-insensitive NCX1.3 mutants. These findings indicate that salt-sensitive hypertension is triggered by Ca^{2+} entry through NCX1 in arterial smooth muscle and suggest that NCX1 inhibitors might be useful therapeutically.

Hypertension is the most common chronic disease, and is the leading risk factor for death that is due to stroke, myocardial infarction or end-stage renal failure^{1,2}. The critical importance of excess salt intake in the pathogenesis of hypertension is widely recognized³⁻⁶, but the mechanism by which excess salt intake elevates blood pressure has puzzled researchers. Recently discovered cardiotonic steroids (CTS), such as endogenous ouabain⁷, and other steroids⁸⁻¹⁰, including marinobufagenin, proscillaridin A and bufalin, have been proposed as candidate intermediaries. In humans, a chronic high-salt diet causes a rise in plasma CTS¹¹⁻¹³. Moreover, ~50% of patients with essential hypertension have substantially elevated levels of endogenous ouabain^{14,15}. Plasma CTS are also high in several salt-dependent hypertensive animals^{7,13,16}. Indeed, PST2238, a ouabain antagonist, lowers blood pressure in salt-dependent hypertensive rats and in certain patients with essential hypertension^{17,18}. Generally, it is believed that CTS inhibit the plasma membrane Na^+/K^+ ATPase, the 'sodium-potassium pump', and lead to an increase in cytosolic Na^+ concentration ($[\text{Na}^+]_{\text{cyt}}$). Cellular Na^+ accumulation raises the cytosolic Ca^{2+} concentration ($[\text{Ca}^{2+}]_{\text{cyt}}$) through the involvement of the $\text{Na}^+/\text{Ca}^{2+}$ exchanger (NCX), and thereby increases contraction in vascular or heart muscle. This may lead to hypertension¹⁹, but the hypothesis has not yet been critically tested because little is understood of the function of NCX in these processes.

NCX is a plasma membrane transporter expressed in various cell types. Membrane potential and transmembrane gradients of Na^+ and Ca^{2+} control this bidirectional exchanger. The mammalian NCX fam-

ily comprises three isoforms²⁰. NCX1 is abundant in the heart, but is also expressed in many other tissues. In contrast, expression of NCX2 and NCX3 is restricted to brain and skeletal muscle. Extensive alternative splicing of NCX1 generates tissue-specific variants²¹⁻²³; the heart expresses exclusively NCX1.1, and vascular tissue predominantly NCX1.3 and NCX1.7. Although the importance of this diversity is unclear, it may reflect different requirements for the maintenance of Ca^{2+} homeostasis in various cell types²⁰. In cardiomyocytes, NCX1 has the primary role in Ca^{2+} extrusion during excitation-contraction coupling²⁴. Under pathological conditions such as cardiac ischemia-reperfusion injury^{25,26}, NCX1 is thought to cause Ca^{2+} overload resulting from elevated $[\text{Na}^+]_{\text{cyt}}$; this leads to cardiac dysfunction. In other tissues, including vascular smooth muscle (VSM), NCX1 is also believed to extrude Ca^{2+} from the cytosol²⁵, but the physiological roles of vascular NCX1 are still unclear.

Recently, SEA0400, a specific NCX inhibitor that preferentially blocks the Ca^{2+} entry mode^{27,28}, was developed. We now report that SEA0400 lowers arterial blood pressure in salt- or ouabain-dependent hypertensive models, but not in normotensive rats or in other types of hypertensive rats. SEA0400 reverses the cytosolic Ca^{2+} elevation and vasoconstriction induced by nanomolar ouabain. Furthermore, we found that heterozygous mice with reduced expression of NCX1 resist development of salt-dependent hypertension. Conversely, transgenic mice with VSM-specific expression of NCX1 readily develop hypertension after high salt intake. These data provide compelling

¹Department of Pharmacology, School of Medicine, Fukuoka University, Fukuoka 814-0180, Japan. ²Department of Physiology, University of Maryland School of Medicine, Baltimore, Maryland 21201, USA. Departments of ³Molecular Physiology and ⁴Bioscience, National Cardiovascular Center Research Institute, Osaka 565-8565, Japan. ⁵Medicinal Research Laboratories, Taisho Pharmaceutical Co., Ltd., Saitama 330-8530, Japan. ⁶Discovery Research Laboratory, Tanabe Seiyaku Co., Ltd., Osaka 532-8505, Japan. ⁷Department of Cardiovascular Science and Medicine, Chiba University Graduate School of Medicine, Chiba 260-8670, Japan. Correspondence should be addressed to T.I. (tiwamoto@cis.fukuoka-u.ac.jp).

Published online 10 October 2004; doi:10.1038/nm1118



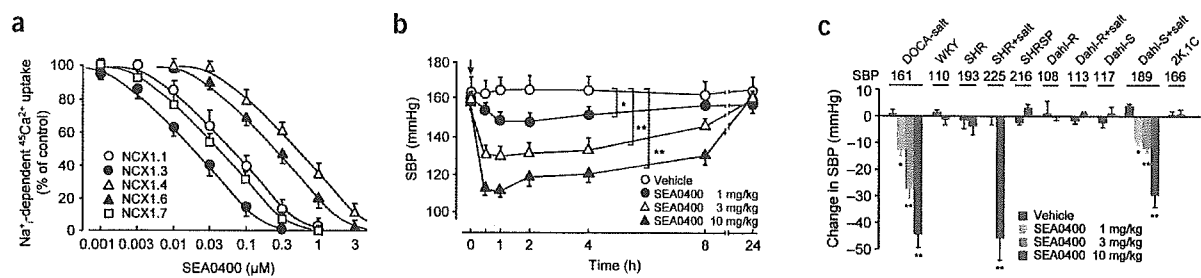


Figure 1 NCX1 inhibition and antihypertensive effects of SEA0400. (a) Concentration-response curves of SEA0400 for intracellular Na⁺ (Na⁺)-dependent ⁴⁵Ca²⁺ uptake into fibroblasts overexpressing variously spliced isoforms of human NCX1. Expression levels and NCX activities in these transfectants are shown in **Supplementary Figure 1** online. (b) Recordings over 24 h (9 a.m. to 9 a.m.) of SBP after oral administration of vehicle or SEA0400 (1–10 mg/kg) in DOCA-salt hypertensive rats. (c) Peak changes in SBP in various types of hypertensive rats treated with oral SEA0400. SHR, Dahl salt-resistant rats (Dahl-R) and Dahl salt-sensitive rats (Dahl-S) were fed a normal (0.3% NaCl) or high-salt diet (8% NaCl; +salt) for 4–6 weeks. Change in SBP in mmHg for the respective rats is indicated. Bars represent means ± s.e.m. (*n* = 4–6). WKY, Wistar Kyoto rats; SHRSP, stroke-prone SHR; 2K,1C, two-kidney, one-clip rats. **P* < 0.05, ***P* < 0.01 compared with each vehicle group.

evidence that salt-dependent hypertension is triggered by Ca²⁺ entry through NCX1 in VSM cells. This finding also suggests that vascular NCX1 is a new therapeutic or diagnostic target for salt-sensitive hypertension.

RESULTS

Antihypertensive effects of SEA0400

In VSM cells, NCX1.3 and NCX1.7 are the dominant splicing isoforms^{21–23}. By measuring intracellular Na⁺-dependent Ca²⁺ uptake into fibroblasts overexpressing splicing isoforms of NCX1, we found that SEA0400, a specific inhibitor for Ca²⁺ entry through NCX1, preferentially blocks the vascular isoforms, especially NCX1.3 (Fig. 1a and **Supplementary Fig. 1** online). This finding indicates that SEA0400 is an excellent pharmacological tool for studying the vascular function of NCX1.

To evaluate the role of NCX1 in hypertension, we tested the effects of SEA0400 on various hypertensive models. A single oral dose of SEA0400 (1–10 mg/kg) caused a dose-dependent and long-lasting decrease in systolic blood pressure (SBP) in deoxycorticosterone acetate (DOCA)-salt hypertensive rats (Fig. 1b). Intravenous administration of SEA0400 (0.3–3 mg/kg) also lowered SBP in anesthetized DOCA-salt hypertensive rats (data not shown). Notably, however, SEA0400 did not significantly affect SBP in spontaneously hypertensive rats (SHR) or Wistar Kyoto rats (*P* > 0.05; Fig. 1c). We also examined the antihypertensive effect of SEA0400 in other hypertensive models. SEA0400 significantly decreased SBP in Dahl salt-sensitive rats and SHR when they were chronically loaded with high salt (*P* < 0.01; Fig. 1c). On the other hand, SEA0400 had no effect on SBP in stroke-prone SHR, salt-loaded or salt-unloaded Dahl salt-resistant rats, salt-unloaded Dahl salt-sensitive rats, or two-kidney, one-clip renal hypertensive rats. Thus, SEA0400 selectively suppresses salt-dependent hypertension.

The effect of chronic treatment with SEA0400 was also tested in DOCA-salt hypertensive rats. Administration of SEA0400 (3 or 10 mg/kg) for 3 weeks efficiently overcame the development of hypertension, vascular hypertrophy and renal dysfunction induced by DOCA-salt treatment (**Supplementary Fig. 2** and **Supplementary Tables 1** and **2** online). This suggests that SEA0400 has therapeutic potential as a new antihypertensive drug.

Direct vasodilation by SEA0400

To analyze its antihypertensive mechanism, we infused SEA0400 into the femoral artery of anesthetized DOCA-salt hypertensive rats

(Fig. 2a). Intrafemoral infusion of SEA0400 (10 μg/kg/min) markedly increased femoral blood flow (FBF), indicating that SEA0400 caused peripheral vasodilation. A similar infusion did not affect FBF in normotensive sham rats. On the other hand, when the femoral artery of the sham rat (recipient) was crossperfused with aortic blood from the DOCA-salt hypertensive rat (donor), the intrafemoral infusion of SEA0400 significantly increased the FBF (*P* < 0.05; Fig. 2b). SEA0400 had no effect in the crossperfusion between two sham rats. This suggests that humoral vasoconstrictors participate in DOCA-salt hypertension; these vasoconstrictor effects can be antagonized by SEA0400.

Endogenous CTS are thought to contribute to the pathogenesis of salt-sensitive hypertension in patients and experimental animals^{7,11–16}. Indeed, chronic administration of ouabain to rats causes hypertension^{29,30}. Therefore, we examined the effect of SEA0400 on ouabain-induced hypertension. SEA0400 (1 or 10 mg/kg) suppressed hypertension in a dose-dependent manner in Sprague-Dawley rats on long-term ouabain treatment (Fig. 3a). SEA0400 did not affect the vasopressor responses to intravenous administration of norepinephrine, angiotensin II and endothelin-1 in anesthetized Sprague-Dawley rats (data not shown). Furthermore, to check the antagonistic interaction between ouabain and SEA0400, either ouabain or SEA0400, or both, were infused into the femoral arteries of anesthetized beagles. Intrafemoral infusion of SEA0400 (50 μg/kg/min) alone did not affect FBF. Infusion of either ouabain (0.5 μg/kg/min), however, reduced the FBF by approximately 50%; addition of SEA0400 then restored FBF to the basal level (Fig. 3b).

Effects of SEA0400 on pressurized small arteries

In VSM cells, inhibition of sarcolemmal Na⁺/K⁺ ATPases by endogenous CTS would be expected to increase [Na⁺]_{cyt} and subsequently to raise [Ca²⁺]_{cyt} through the NCX. To test this hypothesis, we examined the effects of low-dose ouabain and SEA0400 on [Ca²⁺]_{cyt} (measured as fluo-4 fluorescence) and vasoconstriction in intact, pressurized mouse small mesenteric arteries with myogenic tone. Ouabain (100 nM) increased fluo-4 fluorescence by ~12% and myogenic tone by 20–25% (Fig. 4). The physiological consequences of even small changes are profound because of Poiseuille's law³¹: resistance to blood flow, *R*, is inversely proportional to the fourth power of the internal radius, *r* (*R* ∝ 1/*r*⁴). Thus, a 5–10% rise in [Ca²⁺]_{cyt} should augment myogenic tone³² enough to increase *R* (and blood pressure)³¹ by ~20–50% (Fig. 4).

SEA0400 (300 nM) abolished the effects induced by low-dose ouabain. A video clip of the fluo-4 fluorescence data shown in

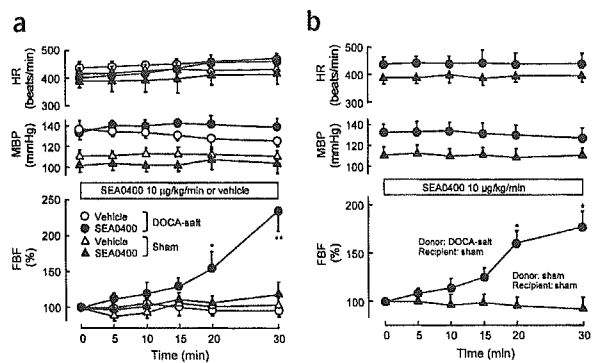


Figure 2 Vascular responses to intrafemoral infusion of SEA0400 in anesthetized DOCA-salt hypertensive or uninephrectomized sham rats. (a) SEA0400 or vehicle was infused at a rate of 20 $\mu\text{l}/\text{min}$ into the femoral artery while monitoring the heart rate (HR), mean blood pressure (MBP), and femoral blood flow (FBF). (b) SEA0400 was infused into the femoral artery of the recipient (sham rat) crossperfused with the blood from the donor (DOCA-salt hypertensive rat or sham rat). Bars represent means \pm s.e.m. ($n = 4$). * $P < 0.05$; ** $P < 0.01$ compared with pretreatment values.

Figure 4b is available online as **Supplementary Movie 1**. In control arteries, SEA0400 also lowered $[\text{Ca}^{2+}]_{\text{cyt}}$ slightly (data not shown) and reduced normal myogenic tone by about 10% (Fig. 4c). SEA0400 had no effect on 75 mM K^+ -induced vasoconstriction (data not shown), consistent with previous reports on SEA0400 selectivity^{27,33}. These results suggest that the increased myogenic tone induced by low-dose ouabain, and even a part of the normal resting tone, may depend upon Ca^{2+} entry mediated by NCX.

Prevention of DOCA-salt hypertension in NCX1 heterozygous mice

To study the functional significance of NCX1 in salt-sensitive hypertension, the hypertensive responsiveness to DOCA-salt treatment was examined in heterozygous NCX1-deficient (*Slc8a1*^{+/-}) mice. The NCX1 protein level in the aorta, as well as in other organs³⁴, of *Slc8a1*^{+/-} mice was about 50% of that seen in wild-type mice (Fig. 5). On the other hand, there were no differences in expression levels of Na^+/K^+ -ATPase (α_2 and α_3), L-type Ca^{2+} channel (α_{1C}) and sarcolemmal Ca^{2+} -ATPase in aortas from *Slc8a1*^{+/-} mice (data not shown). Basal SBP of *Slc8a1*^{+/-} mice was no different from that of wild-type mice. DOCA-salt treatment produced a progressive elevation in SBP in wild-type mice ($P < 0.01$), whereas the same treatment did not significantly alter the SBP of *Slc8a1*^{+/-} mice ($P > 0.05$; Fig. 5a). When the sodium level in drinking water for DOCA-salt treatment was increased from 1% to 2%, *Slc8a1*^{+/-} mice responded with a mild increase in SBP (108 ± 3 mmHg ($n = 5$) at 3 weeks, $P < 0.05$), though wild-type mice experienced severe hypertension (128 ± 5 mmHg ($n = 5$), $P < 0.01$). In contrast, hypertensive responses to chronic angiotensin II infusion were similar in *Slc8a1*^{+/-} and wild-type mice (Fig. 5b).

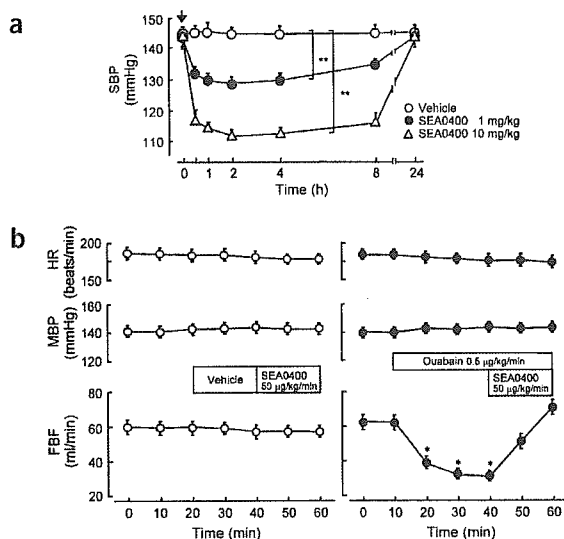


Salt hypersensitivity in VSM-specific NCX1.3 transgenic mice

To test further whether vascular NCX1 has a critical role in salt-sensitive hypertension, we created transgenic mice (*NI.3^{Tg/Tg}*) expressing canine *Ncx1.3* driven by the smooth muscle α -actin promoter (Fig. 6a). Southern blotting indicated that four founders had 2–4 copies of the transgene (data not shown). From among them, two independent transgenic lines were selected for detailed study. Western blot analysis showed that NCX1.3 protein was overexpressed in the aortas, but not in the hearts, of these transgenic mice at 6- to 8-fold the level of endogenous NCX1 (Supplementary Fig. 3 online). Immunohistochemical staining indicated dense localization of NCX1.3 in the medial layer of aortas from *NI.3^{Tg/Tg}* mice (Fig. 6b). On the other hand, no difference was observed in protein levels of Na^+/K^+ -ATPase (α_2 and α_3), L-type Ca^{2+} channel (α_{1C}) and sarcolemmal Ca^{2+} -ATPase in aortas from *NI.3^{Tg/Tg}* mice by western blotting (data not shown). Functional augmentation was correlated with increased NCX1 protein levels in aortas from *NI.3^{Tg/Tg}* mice, as shown by measuring the rate and degree of contraction evoked by Na^+ removal in aortic rings pretreated with ouabain (Supplementary Fig. 3 online). Furthermore, the 10 μM ouabain-induced $[\text{Ca}^{2+}]_{\text{cyt}}$ rise in mesenteric arteries from *NI.3^{Tg/Tg}* mice was notably greater than in those from wild-type mice (Fig. 6c,d).

Notably, the basal SBP of *NI.3^{Tg/Tg}* mice (103 ± 1.4 mmHg, $n = 6$) was slightly, but significantly ($P < 0.05$), higher than that of wild-type mice (92 ± 1.1 mmHg, $n = 5$). When these mice were fed an 8% NaCl diet with 1% NaCl drinking water, SBP in *NI.3^{Tg/Tg}* mice, but not in wild-type mice, progressively rose to 124 ± 3.5 mmHg ($n = 6$) at 4 weeks after the start of salt loading (Fig. 6e). Oral administration of SEA0400 (10 mg/kg) markedly lowered the SBP of salt-loaded *NI.3^{Tg/Tg}* mice, but not of salt-loaded wild-type mice (Fig. 6f). Intravenous administration of SEA0400 (0.3 mg/kg) also lowered SBP in anesthetized *NI.3^{Tg/Tg}* mice by about 20 mmHg (data not shown). In addition, oral administration of SEA0400 suppressed basal SBP (mild hypertension) of *NI.3^{Tg/Tg}* mice, but not of wild-type mice, and abolished the difference between the two groups (Supplementary Fig. 3 online).

Figure 3 Effects of SEA0400 on ouabain-induced hypertension and vasoconstriction. (a) Recordings over 24 h of SBP after oral administration of SEA0400 in hypertensive rats infused subcutaneously with ouabain (30 $\mu\text{g}/\text{kg}/\text{d}$ for 5 weeks). ** $P < 0.01$ compared with the vehicle group ($n = 5$). (b) Femoral blood flow (FBF) response to intrafemoral infusion of SEA0400 or vehicle at a rate of 0.2 ml/kg/min in the presence (right) or absence (left) of ouabain in anesthetized beagles. MBP and HR were monitored during the experimental periods. * $P < 0.05$ compared with pretreatment values ($n = 4$).



ARTICLES

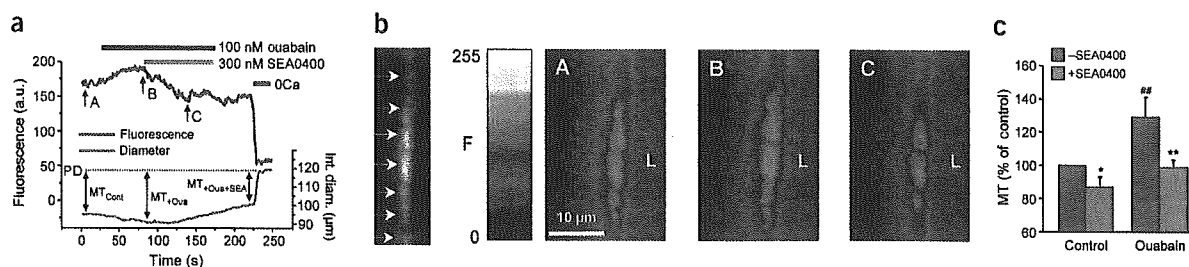


Figure 4 Effects of low-dose ouabain and SEA0400 on cytosolic Ca^{2+} level and myogenic tone (MT) in pressurized mouse small mesenteric arteries. (a) Simultaneous recording of fluorescence and internal diameter (Int. diam.) changes in a fluo-4 loaded artery (pressurized to 70 mmHg) by laser confocal microscopy. The fluo-4 fluorescence, indicated in arbitrary units (a.u.), reflects $[\text{Ca}^{2+}]_{\text{cyt}}$. Periods of exposure to ouabain, SEA0400 and Ca^{2+} -free medium (OCa) are indicated by colored bars. The dotted line shows the passive internal diameter (PD) in OCa. (b) Fluorescent image on the left shows individual myocytes loaded with fluo-4 (arrows); the artery has only a single layer of myocytes. Pseudocolor images (A–C) indicate the relative $[\text{Ca}^{2+}]_{\text{cyt}}$ at the times shown in a. L, artery lumen. A video clip of the original data from this experiment is available at **Supplementary Movie 1** online. (c) Summary of the effects of ouabain and SEA0400 on MT, normalized to MT under control conditions. Mean PD was $107 \pm 4 \mu\text{m}$. At 70 mmHg, arteries constricted to $77 \pm 4 \mu\text{m}$ internal diameter (= control MT). Ouabain caused a further constriction to $70 \pm 4 \mu\text{m}$; based on Poiseuille's law³¹, this should increase resistance to blood flow (and blood pressure) by ~46%. * $P < 0.05$; ** $P < 0.01$ versus pretreatment values ('-SEA0400'). ## $P < 0.01$ versus control values ($n = 6$).

To verify that the antihypertensive effect of SEA0400 results from the inhibition of genetically overexpressed NCX1.3, we generated transgenic mice ($mN1.3^{\text{Tg/Tg}}$) expressing an SEA0400-insensitive G833C mutant²⁸ (Fig. 6a). Three independent lines of $mN1.3^{\text{Tg/Tg}}$ mice were selected for detailed analysis. The phenotypes of $mN1.3^{\text{Tg/Tg}}$ mice were very similar to those of $N1.3^{\text{Tg/Tg}}$ mice, except for their vascular response to SEA0400 (Fig. 6b–e and **Supplementary Fig. 3** online); this drug blocked the contraction evoked by Na^+ removal in ouabain-pretreated aortic rings and the ouabain-induced $[\text{Ca}^{2+}]_{\text{cyt}}$ rise in arterial strips from $N1.3^{\text{Tg/Tg}}$ mice, but not from $mN1.3^{\text{Tg/Tg}}$ mice. In $mN1.3^{\text{Tg/Tg}}$ mice, SEA0400 (10 mg/kg) did not show a reduction in high salt-induced hypertension (Fig. 6f) and basal SBP (**Supplementary Fig. 3** online). This shows that SEA0400 acts on the overexpressed NCX1.3 in VSM cells.

Given the possibility of nonspecific effects associated with NCX1 overexpression, as a further control we generated transgenic mice ($N1.1^{\text{Tg/Tg}}$) expressing canine *Ncx1.1* driven by the α -myosin heavy-chain promoter. In established $N1.1^{\text{Tg/Tg}}$ lines, hearts, but not aortas, showed a 2- to 3-fold increase in the level of NCX1 protein. Basal SBP of $N1.1^{\text{Tg/Tg}}$ mice was normal, and was similar to that of wild-type mice. Furthermore, the blood pressure of $N1.1^{\text{Tg/Tg}}$ mice, like that of wild-type mice, was resistant to long-term salt-loading and insensitive to the effect of SEA0400 (**Supplementary Fig. 4** online).

DISCUSSION

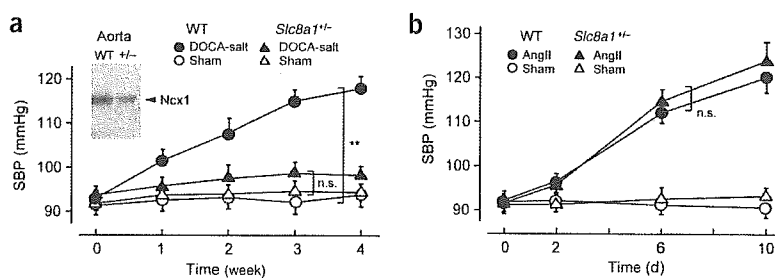
The critical importance of sodium retention, resulting from excess salt intake or reduced renal salt excretion, in the pathogenesis of

hypertension is widely recognized^{3–6}. But the molecular mechanisms underlying salt-sensitive hypertension remain obscure. Here we show that SEA0400 lowers arterial blood pressure in various models of salt-dependent hypertension. SEA0400 does not, however, affect arterial blood pressure in normotensive rats or in other types of hypertensive rats. Furthermore, NCX1 heterozygous mice are resistant to DOCA-salt hypertension, but not to angiotensin II-induced hypertension. These findings suggest that vascular NCX1 is critical in the development of salt-sensitive hypertension.

The contraction of VSM cells is initiated by a rise in $[\text{Ca}^{2+}]_{\text{cyt}}$ through voltage-gated or receptor-operated Ca^{2+} channels in the sarcolemma, or both, or through Ca^{2+} -release channels in the sarcoplasmic reticulum membrane^{35,36}. In general, sarcolemmal NCX, like the sarcolemmal or sarcoplasmic reticulum Ca^{2+} -ATPases, is thought to contribute to Ca^{2+} extrusion from the cytosol in the relaxation process. Data obtained using antisense oligonucleotides indicate that NCX1 knockdown prolongs agonist responses by delaying the return of $[\text{Ca}^{2+}]_{\text{cyt}}$ to the resting level in cultured VSM cells^{37,38}.

To confirm the *in vivo* function of vascular NCX1 in mice, we generated VSM-specific transgenic mice expressing either wild-type NCX1.3 ($N1.3^{\text{Tg/Tg}}$) or the SEA0400-insensitive G833C mutant ($mN1.3^{\text{Tg/Tg}}$). Comparative experiments using these mutants and SEA0400 are useful for assessing the pharmacological significance of NCX inhibition²⁸. Interestingly, both kinds of transgenic mice were mildly hypertensive (by about 10 mmHg) compared with wild-type mice. They also exhibited high salt-induced hypertension as a result of increased salt sensitivity. Administration of SEA0400 normalized

Figure 5 Prevention of DOCA-salt hypertension in $Slc8a1^{+/-}$ mice. (a) Uninephrectomized $Slc8a1^{+/-}$ and wild-type (WT) mice received DOCA (75 mg/kg) subcutaneously twice a week, and were given tap water containing 1% NaCl for 4 weeks. Sham mice were uninephrectomized but not given DOCA and salt. (b) Miniosmotic pumps containing angiotensin II (AngII) or vehicle (sham) were subcutaneously implanted in $Slc8a1^{+/-}$ and WT mice on day 0. Systolic blood pressure (SBP) was monitored by tail cuff. ** $P < 0.01$ versus control groups ($n = 5$ or 6).





blood pressure and suppressed salt-dependent hypertension in *N1.3^{Tg/Tg}* mice, but not in *mN1.3^{Tg/Tg}* mice. The latter mutation interferes with SEA0400 binding but does not affect $\text{Na}^+/\text{Ca}^{2+}$ exchange²⁸. In contrast, heart-specific transgenic mice expressing NCX1.1 were salt-insensitive, and their blood pressure did not respond to SEA0400. These results indicate that vascular NCX1 acts primarily as a Ca^{2+} entry pathway for regulating arterial tone, especially under sodium-retaining conditions. SEA0400 exerts its antihypertensive effect by blocking this Ca^{2+} entry in arterial myocytes.

Indeed, SEA0400 reverses the vasoconstriction and hypertension induced by exogenous ouabain, which may facilitate Ca^{2+} entry through NCX due to elevated $[\text{Na}^+]_{\text{cyt}}$ although SEA0400 does not directly affect the activity of $\text{Na}^+/\text{K}^+-\text{ATPases}$ ²⁷. Notably, in VSM cells the NCX1 is colocalized with $\text{Na}^+/\text{K}^+-\text{ATPase}$ α_2 and α_3 isoforms, which have high affinity for ouabain³⁹, in plasma membrane microdomains adjacent to the sarcoplasmic reticulum^{40,41}. Functional coupling between NCX and $\text{Na}^+/\text{K}^+-\text{ATPase}$ has been reported in vascular and cardiac myocytes^{37,42–44}. As described above, endogenous plasma CTS are increased under pathological conditions such as salt-sensitive hypertension^{7,11–16}. When CTS inhibit $\text{Na}^+/\text{K}^+-\text{ATPases}$ (α_2 and α_3) in VSM cells, the elevation of local Na^+ in the submembrane area is expected to facilitate Ca^{2+} entry through NCX1, resulting in vasoconstriction. Our data indicate that blood from DOCA-salt hypertensive rats contains humoral vasoconstrictors whose action is counteracted by SEA0400. Also, using isolated, pressurized mouse small mesenteric arteries, we confirmed that 100 nM ouabain increases both $[\text{Ca}^{2+}]_{\text{cyt}}$ and myogenic tone by about 20–25% and that SEA0400 completely abolishes these effects. In addition, the 10 μM ouabain-induced $[\text{Ca}^{2+}]_{\text{cyt}}$ rise in arterial strips from transgenic mice was greater than in those from wild-type mice. SEA0400 blocked these $[\text{Ca}^{2+}]_{\text{cyt}}$ rises in *N1.3^{Tg/Tg}* and wild-type mice, but not in *mN1.3^{Tg/Tg}* mice. These data provide evidence that ouabain triggers Ca^{2+} entry through NCX1 in VSM cells by inhibiting high ouabain-affinity Na^+ pumps (α_2 or α_3) and elevating submembrane Na^+ . Although ouabain has also been reported to mediate other signaling pathways⁴⁵, they apparently are not involved in the VSM mechanism described here.

SEA0400 does not affect arterial blood pressure in normotensive or salt-independent hypertensive animals. Intrafemoral infusion of SEA0400 in normal rats and beagles does not change arterial blood flow unless the arteries are perfused with exogenous ouabain or aortic blood from salt-dependent hypertensive animals. In addition, NCX1 heterozygous mice maintain normal blood pressure. Thus, the Ca^{2+} entry mode of NCX1 in VSM cells apparently has little role in blood pressure control in normotensive or in salt-insensitive hypertensive

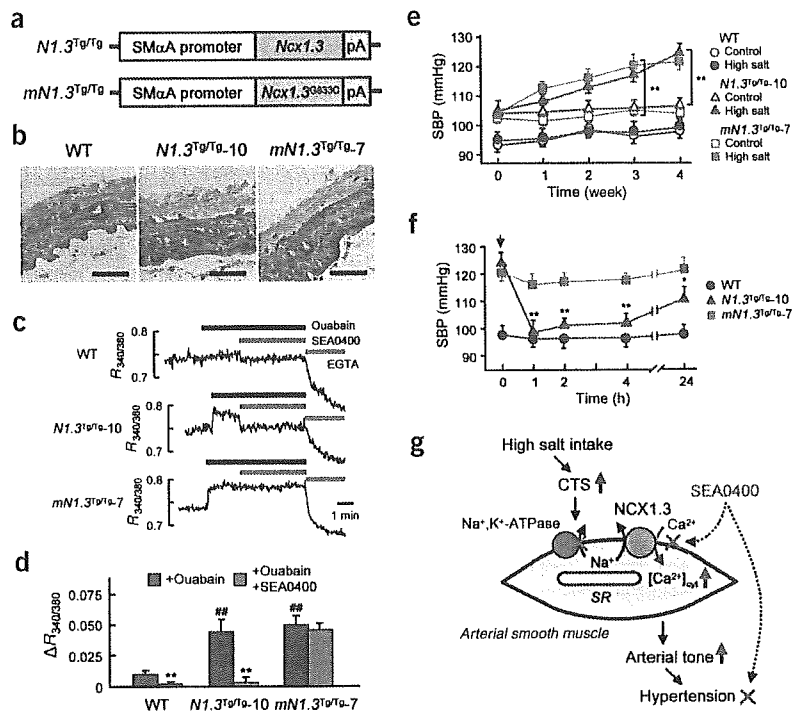


Figure 6 Enhanced salt-sensitivity in *N1.3^{Tg/Tg}* or *mN1.3^{Tg/Tg}* mice. (a) Schematic representation of the transgene used to generate VSM-specific transgenic mice. The *Ncx1.3* or its G833C mutant (*Ncx1.3^{G833C}*) was brought under the control of human smooth muscle α -actin (SM α A) promoter. (b) Immunohistochemical localization of NCX1 proteins in the medial layer of thoracic aortas from wild-type (WT) mice and two representative transgenic lines (*N1.3^{Tg/Tg-10}* and *mN1.3^{Tg/Tg-7}*). Scale bars, 50 μm . (c) Effects of ouabain and SEA0400 on $[\text{Ca}^{2+}]_{\text{cyt}}$ (fura-PE3 fluorescence ratio ($R_{340/380}$)) in isolated mesenteric arteries from transgenic and WT mice. Periods of exposure to 10 μM ouabain, 1 μM SEA0400 and 4 mM EGTA are indicated by bars. All experiments were performed in the presence of 10 μM nifedipine to suppress L-type Ca^{2+} channels. (d) Summary of the experiments shown in (c). ** $P < 0.01$ versus pretreatment values ('+Ouabain'). ## $P < 0.01$ versus WT groups ($n = 5$). (e, f) Salt-induced hypertension and antihypertensive effects of SEA0400 (10 mg/kg) in transgenic and WT mice treated with a high-salt diet (8% NaCl) and tap water containing 1% NaCl for 4 weeks. * $P < 0.05$; ** $P < 0.01$ ($n = 5$ or 6). (g) Proposed pathway responsible for salt-sensitive hypertension. High salt intake causes the levels of endogenous CTS to rise in the plasma. This results in the increase in subplasma membrane $[\text{Na}^+]_{\text{cyt}}$ of arterial smooth muscle. The restricted $[\text{Na}^+]_{\text{cyt}}$ accumulation elevates $[\text{Ca}^{2+}]_{\text{cyt}}$ by vascular NCX1 isoform-mediated Ca^{2+} entry. This enhances arterial tone and causes hypertension. SEA0400 blocks this Ca^{2+} entry and exerts an antihypertensive effect in salt-sensitive hypertension.

animals, probably owing to low plasma levels of CTS and to the overriding effects of reflex regulatory mechanisms. Nevertheless, the Ca^{2+} entry mode of NCX1 could have a role in regional blood flow even in normotensive and salt-insensitive animals, because SEA0400 slightly suppresses basal myogenic tone with a small reduction of $[\text{Ca}^{2+}]_{\text{cyt}}$ in pressurized mouse small mesenteric arteries.

In conclusion, our results show that the Ca^{2+} entry mode of vascular NCX1 is involved in the contractile regulation of small arteries and in the development of salt-dependent hypertension. Notably, recent human genome-wide linkage analysis of genes that affect blood pressure identified four regions, one of which includes *SLC8A1*, as loci containing candidate genes that influence blood pressure⁴⁶. In humans and animals, endogenous CTS levels increase in plasma during salt retention^{7,11–16}. Inhibition of Na^+ pumps by CTS should elevate local Na^+ and, through NCX1, $[\text{Ca}^{2+}]_{\text{cyt}}$ in VSM cells, thereby

ARTICLES

promoting vasoconstriction (Fig. 6g). In this pathway, vascular NCX1 is a key mediator. SEA0400 selectively blocks NCX1.3, the vascular isoform of NCX1, and suppresses salt-dependent hypertension and associated secondary organ damage. Thus, the Ca^{2+} entry mode of vascular NCX1 may be a useful target for the development of therapies for salt-sensitive hypertension. Indeed, response to inhibitors of NCX1 may be diagnostic for salt-sensitive hypertension and involvement of the pathway illustrated in Figure 6g.

METHODS

$^{45}\text{Ca}^{2+}$ uptake. To examine the splice isoform selectivity of SEA0400, we cloned *NCX1.1*, *NCX1.3*, *NCX1.4*, *NCX1.6* and *NCX1.7* into pcDNA3.1 (Invitrogen) by PCR using human aortic cDNAs (Clontech). We transfected these plasmids with Lipofectin (Invitrogen) into CCL39 fibroblasts and we selected cells stably expressing NCX1 using a Ca^{2+} -killing procedure¹⁷. Intracellular Na^+ -dependent $^{45}\text{Ca}^{2+}$ uptake into cells was assayed as described⁴⁷ (see Supplementary Methods online).

Experimental hypertensive models. To produce DOCA-salt hypertensive animals, 5-week-old male Sprague-Dawley rats or 12-week-old male mice were unilaterally nephrectomized under anesthesia with sodium pentobarbital. After allowing the animals a 1-week recovery, we administered DOCA (15 mg/kg for rats or 75 mg/kg for mice) with corn oil subcutaneously twice a week for 4 weeks. These animals then drank tap water containing 1% NaCl. Control animals (sham) were uninephrectomized but not given DOCA and salt. In the preparation of two-kidney, one-clip renal hypertensive rats, we anesthetized male Sprague-Dawley rats with sodium pentobarbital, and partially occluded the left renal artery by a silver clip (0.2 mm in diameter) for 4 weeks. To produce ouabain-induced hypertension, we infused ouabain subcutaneously at a rate of 30 $\mu\text{g}/\text{kg}/\text{day}$ into male Sprague-Dawley rats by miniosmotic pumps (ALZET 2002) for 5 weeks. Ouabain was dissolved in sterile phosphate-buffered saline. To produce angiotensin II-induced hypertension, we subcutaneously implanted miniosmotic pumps containing either vehicle (0.01 N acetic acid in saline solution) or angiotensin II (750 $\mu\text{g}/\text{kg}/\text{d}$ for 10 d) in male mice. We measured SBP at room temperature by a tail cuff method using an MK2000 blood pressure monitor (Muromachi Kikai). Rats or mice were acclimated to the procedures of blood pressure measurement for a week preceding actual data collection. We administered SEA0400 orally or intravenously with 5% gum arabic or a lipid emulsion containing 20% soybean oil (vehicle), respectively.

Intrafemoral infusion. To determine the peripheral vasodilation, we infused SEA0400 (10 $\mu\text{g}/\text{kg}/\text{min}$) or vehicle at a rate of 20 $\mu\text{l}/\text{min}$ through a polyethylene tube in the right femoral artery of DOCA-salt hypertensive rats or uninephrectomized sham rats, anesthetized with sodium pentobarbital. In other experiments, we infused SEA0400 into the right femoral artery of the sham rat (recipient), which was crossperfused with vena caval and aortic blood of the donor rat and stabilized for 30 min. In yet other experiments, we infused SEA0400 (50 $\mu\text{g}/\text{kg}/\text{min}$) alone or in combination with ouabain (0.5 $\mu\text{g}/\text{kg}/\text{min}$) at a rate of 0.2 ml/min into the left femoral artery of anesthetized male beagles (9–10 kg). In all these experiments, FBF, systemic blood pressure and heart rate were monitored directly with a square-wave flowmeter and a pressure transducer (Nihon Koden), respectively.

Transgenic mice. We constructed the transgene by inserting canine *Ncx1.3* or its G833C mutant²⁸ between the human smooth muscle α -actin promoter and the SV40 polyadenylation sequence of the plasmid (T. Miwa). We also prepared an additional transgene by inserting canine *Ncx1.1* between the mouse α -myosin heavy chain promoter and the SV40 polyadenylation sequence of the plasmid (J. Robbins). Each transgene was microinjected into the pronuclei of fertilized C57BL/6j mouse embryos at the single-cell stage. We implanted the embryos into pseudopregnant foster mothers. Positive transgenic mice were identified as described³⁴; mice were bred to homozygosity.

Imaging of small mesenteric arteries. Diameter measurement and Ca^{2+} imaging of mouse mesenteric artery were performed as described⁴⁸. Distal mesenteric arteries (2–3 mm length, 120–150 μm passive external diameter) from

male C57BL/6j mice were cannulated at both ends and continuously superfused with gassed Krebs solution (37 °C, 70 mmHg) to induce myogenic tone. For measurement of diameter only, the artery outer diameter was continuously monitored by a real-time edge-detection system (National Instruments). For Ca^{2+} imaging, arterial segments were loaded with 15 μM fluo-4-AM for ~3 h. We imaged dye-loaded arteries with a confocal imaging system (Nipkow-Yokogawa dual spinning disk, Solamere Technology) connected to a Nikon Eclipse 2000 microscope equipped with a water immersion objective ($\times 60$). Images were captured at the rate of 2–4 frames/s.

Other procedures and materials. Immunoblotting for membrane proteins and immunohistochemistry of frozen sections were performed as described^{47,49}, with some modifications. We performed analyses of aortic morphology and renal function as described⁵⁰. We also performed measurements of contraction in aortic rings and $[\text{Ca}^{2+}]_{\text{cyt}}$ (fura-PE3 fluorescence ratio; $R_{340/380}$) in arterial strips as described^{34,38}, with some modifications (see Supplementary Methods online). We used an unpaired *t*-test, one-way ANOVA followed by Dunnett's test or two-way ANOVA for statistical analyses. Values of $P < 0.05$ were considered statistically significant. SEA0400 (2-[4-[(2,5-difluorophenyl)methoxy]phenoxy]-5-ethoxyaniline) was synthesized by Taisho Pharmaceutical Co. Ltd.

Animal regulations. We used all animals in accordance with the Guidelines for Animal Experiments in Fukuoka University and the US National Institutes of Health Guide for the Care and Use of Laboratory Animals.

Note: Supplementary information is available on the Nature Medicine website.

ACKNOWLEDGMENTS

We thank K. Takahashi and S. Okuyama (Taisho Pharmaceutical Co. Ltd.), K. Saku and H. Urata (Fukuoka University), J. Kimura (Fukushima Medical University) and Y. Matsumura (Osaka University of Pharmaceutical Sciences) for discussions, and W.G. Wier and R. Saunders (University of Maryland) for help in making the video clip. This work was supported by Grants-in-Aid for scientific research (14570097, 16590213) from the Ministry of Education, Science and Culture of Japan, a grant from the Salt Science Research Foundation (No.02), US National Institutes of Health grant HL-45215, and an American Heart Association Mid-Atlantic Affiliate Postdoctoral Fellowship.

COMPETING INTERESTS STATEMENT

The authors declare that they have no competing financial interests.

Received 20 May; accepted 8 September 2004

Published online at <http://www.nature.com/naturemedicine/>

1. Mosterd, A. *et al.* Trends in the prevalence of hypertension, antihypertensive therapy, and left ventricular hypertrophy from 1950 to 1989. *N. Engl. J. Med.* **340**, 1221–1227 (1999).
2. Kannel, W.B. Elevated systolic blood pressure as a cardiovascular risk factor. *Am. J. Cardiol.* **85**, 251–255 (2000).
3. Cowley, A.W. Long-term control of arterial blood pressure. *Physiol. Rev.* **72**, 231–300 (1992).
4. Blaustein, M.P. Physiological effects of endogenous ouabain: control of intracellular calcium stores and cell responsiveness. *Am. J. Physiol.* **264**, C1367–C1387 (1993).
5. Haddy, F.J. & Pamnani, M.B. Role of dietary salt in hypertension. *J. Am. Coll. Nutr.* **14**, 428–438 (1995).
6. Lifton, R.P., Gharavi, A.G. & Geller, D.S. Molecular mechanisms of human hypertension. *Cell* **104**, 545–556 (2001).
7. Hamlyn, J.M. *et al.* Identification and characterization of a ouabain-like compound from human plasma. *Proc. Natl. Acad. Sci. USA* **88**, 6259–6263 (1991).
8. Schneider, R. *et al.* Bovine adrenals contain, in addition to ouabain, a second inhibitor of the sodium pump. *J. Biol. Chem.* **273**, 784–792 (1998).
9. Bagrov, A.Y. *et al.* Characterization of a urinary bufodienolide Na^+/K^+ -ATPase inhibitor in patients after acute myocardial infarction. *Hypertension* **31**, 1097–1103 (1998).
10. Schoner, W. Endogenous cardiac glycosides, a new class of steroid hormones. *Eur. J. Biochem.* **269**, 2440–2448 (2002).
11. Hamlyn, J.M. *et al.* A circulating inhibitor of (Na^+/K^+) -ATPase associated with essential hypertension. *Nature* **300**, 650–652 (1982).
12. Hasegawa, T., Masugi, F., Ogihara, T. & Kumahara, Y. Increase in plasma ouabain-like inhibitor of Na^+/K^+ -ATPase with high sodium intake in patients with essential hypertension. *J. Clin. Hypertens.* **3**, 419–429 (1987).
13. Hamlyn, J.M., Hamilton, B.P. & Manunta, P. Endogenous ouabain, sodium balance and blood pressure: a review and a hypothesis. *J. Hypertens.* **14**, 151–167 (1996).



14. Manunta, P. *et al.* Left ventricular mass, stroke volume, and ouabain-like factor in essential hypertension. *Hypertension* **34**, 450–456 (1999).
15. Goto, A. & Yamada, K. Putative roles of ouabainlike compound in hypertension: revisited. *Hypertens. Res.* **23**, S7–S13. (2000).
16. Fedorova, O.V., Lakatta, E.G. & Bagrov, A.Y. Endogenous Na,K pump ligands are differentially regulated during acute NaCl loading of Dahl rats. *Circulation* **102**, 3009–3014 (2000).
17. Ferrari, P. *et al.* PST2238: a new antihypertensive compound that antagonizes the long-term pressor effect of ouabain. *J. Pharmacol. Exp. Ther.* **285**, 83–94 (1998).
18. Takahashi, H. Endogenous digitalislike factor: an update. *Hypertens. Res.* **23**, S1–S5 (2000).
19. Blaustein, M.P. Sodium ions, calcium ions, blood pressure regulation, and hypertension: a reassessment and a hypothesis. *Am. J. Physiol.* **232**, C165–C173 (1977).
20. Philipson, K.D. & Nicoll, D.A. Sodium-calcium exchange: a molecular perspective. *Annu. Rev. Physiol.* **62**, 111–133. (2000).
21. Nakasaki, Y., Iwamoto, T., Hanada, H., Imagawa, T. & Shigekawa, M. Cloning of the rat aortic smooth muscle Na⁺/Ca²⁺ exchanger and tissue-specific expression of isoforms. *J. Biochem.* **114**, 528–534 (1993).
22. Lee, S.L., Yu, A.S. & Lytton, J. Tissue-specific expression of Na⁺-Ca²⁺ exchanger isoforms. *J. Biol. Chem.* **269**, 14849–14852 (1994).
23. Quednau, B.D., Nicoll, D.A. & Philipson, K.D. Tissue specificity and alternative splicing of the Na⁺/Ca²⁺ exchanger isoforms NCX1, NCX2, and NCX3 in rat. *Am. J. Physiol.* **272**, C1250–C1261 (1997).
24. Bers, D.M. Cardiac excitation-contraction coupling. *Nature* **415**, 198–205 (2002).
25. Blaustein, M.P. & Lederer, W.J. Sodium/calcium exchange: its physiological implications. *Physiol. Rev.* **79**, 763–854 (1999).
26. Shigekawa, M. & Iwamoto, T. Cardiac Na⁺-Ca²⁺ exchange: molecular and pharmacological aspects. *Circ. Res.* **88**, 864–876 (2001).
27. Matsuda, T. *et al.* SEA0400, a novel and selective inhibitor of the Na⁺-Ca²⁺ exchanger, attenuates reperfusion injury in the in vitro and in vivo cerebral ischemic models. *J. Pharmacol. Exp. Ther.* **298**, 249–256 (2001).
28. Iwamoto, T. *et al.* Molecular determinants of Na⁺/Ca²⁺ exchange (NCX1) inhibition by SEA0400. *J. Biol. Chem.* **279**, 7544–7553 (2004).
29. Yuan, C.M. *et al.* Long-term ouabain administration produces hypertension in rats. *Hypertension* **22**, 178–187 (1993).
30. Manunta, P., Rogowski, A.C., Hamilton, B.P. & Hamlyn, J.M. Ouabain-induced hypertension in the rat: relationships among plasma and tissue ouabain and blood pressure. *J. Hypertens.* **12**, 549–560 (1994).
31. Berne, R.M. & Levy, M.N. Chapter V. Hemodynamics. in *Cardiovascular Physiology* edn. 8 (eds. Berne, R.M. & Levy, M.N.) 115–134 (Mosby, St. Louis, 2001).
32. Knot, H.J. & Nelson, M.T. Regulation of arterial diameter and wall [Ca²⁺] in cerebral arteries of rat by membrane potential and intravascular pressure. *J. Physiol.* **508**, 199–209 (1998).
33. Tanaka, H. *et al.* Effect of SEA0400, a novel inhibitor of sodium-calcium exchanger, on myocardial ionic currents. *Br. J. Pharmacol.* **135**, 1096–1100 (2002).
34. Wakimoto, K. *et al.* Targeted disruption of Na⁺/Ca²⁺ exchanger gene leads to cardiomyocyte apoptosis and defects in heartbeat. *J. Biol. Chem.* **275**, 36991–36998 (2000).
35. Berridge, M.J., Bootman, M.D. & Roderick, H.L. Calcium signalling: dynamics, homeostasis and remodelling. *Nat. Rev. Mol. Cell Biol.* **4**, 517–529 (2003).
36. Poburko, D., Kuo, K.H., Dai, J., Lee, C.H. & van Breemen, C. Organellar junctions promote targeted Ca²⁺ signaling in smooth muscle: why two membranes are better than one. *Trends Pharmacol. Sci.* **25**, 8–15 (2004).
37. Slodzinski, M.K., Juhaszova, M. & Blaustein, M.P. Antisense inhibition of Na⁺/Ca²⁺ exchange in primary cultured arterial myocytes. *Am. J. Physiol.* **269**, C1340–C1345 (1995).
38. Slodzinski, M.K. & Blaustein, M.P. Physiological effects of Na⁺/Ca²⁺ exchanger knockdown by antisense oligodeoxynucleotides in arterial myocytes. *Am. J. Physiol.* **275**, C251–C259 (1998).
39. Sweadner, K.J. Isozymes of the Na⁺/K⁺-ATPase. *Biochim. Biophys. Acta.* **988**, 185–220 (1989).
40. Moore, E.D. *et al.* Coupling of the Na⁺/Ca²⁺ exchanger, Na⁺/K⁺ pump and sarcoplasmic reticulum in smooth muscle. *Nature* **365**, 657–660 (1993).
41. Juhaszova, M. & Blaustein, M.P. Distinct distribution of different Na⁺ pump α subunit isoforms in plasmalemma. Physiological implications. *Ann. N.Y. Acad. Sci.* **834**, 524–536 (1997).
42. Fujioka, Y., Matsuoka, S., Ban, T. & Noma, A. Interaction of the Na⁺-K⁺ pump and Na⁺-Ca²⁺ exchange via [Na⁺]_i in a restricted space of guinea-pig ventricular cells. *J. Physiol.* **509**, 457–470 (1998).
43. Arnon, A., Hamlyn, J.M. & Blaustein, M.P. Ouabain augments Ca²⁺ transients in arterial smooth muscle without raising cytosolic Na⁺. *Am. J. Physiol.* **279**, H679–H691 (2000).
44. Reuter, H. *et al.* The Na⁺-Ca²⁺ exchanger is essential for the action of cardiac glycosides. *Circ. Res.* **90**, 305–308 (2002).
45. Aizman, O., Uhlen, P., Lal, M., Brismar, H. & Aperia, A. Ouabain, a steroid hormone that signals with slow calcium oscillations. *Proc. Natl. Acad. Sci. USA* **98**, 13420–13424 (2001).
46. Krushkal, J. *et al.* Genome-wide linkage analyses of systolic blood pressure using highly discordant siblings. *Circulation* **99**, 1407–1410 (1999).
47. Iwamoto, T., Pan, Y., Nakamura, T.Y., Wakabayashi, S. & Shigekawa, M. Protein kinase C-dependent regulation of Na⁺/Ca²⁺ exchanger isoforms NCX1 and NCX3 does not require their direct phosphorylation. *Biochemistry* **37**, 17230–17238 (1998).
48. Zhang, J., Wier, W.G. & Blaustein, M.P. Mg²⁺ blocks myogenic tone but not K⁺-induced constriction: role for SOCs in small arteries. *Am. J. Physiol.* **283**, H2692–H2705 (2002).
49. Yamashita, J. *et al.* Attenuation of ischemia/reperfusion-induced renal injury in mice deficient in Na⁺/Ca²⁺ exchanger. *J. Pharmacol. Exp. Ther.* **304**, 284–293 (2003).
50. Matsumura, Y. *et al.* Exaggerated vascular and renal pathology in endothelin-B receptor-deficient rats with deoxycorticosterone acetate-salt hypertension. *Circulation* **102**, 2765–2773 (2000).

